

Electrostatic Properties of Membranes: The Poisson–Boltzmann Theory

D. ANDELMAN

*School of Physics and Astronomy, Tel Aviv University,
Ramat Aviv 69978, Tel Aviv, Israel*

Contents

1. Introduction	605
2. Charged surfaces in liquids: general considerations	607
2.1. Poisson–Boltzmann equation	608
2.2. Electrostatic free energy and electrostatic pressure	610
2.3. Beyond Poisson–Boltzmann: recent theory and experiment	611
3. A single flat and charged membrane	612
3.1. No added electrolyte	612
3.2. Added electrolyte	613
4. Two flat charged membranes	614
4.1. No added electrolyte	615
4.2. Added electrolyte	617
5. Flexible and charged membranes: general considerations	622
6. A single charged and flexible membrane	623
6.1. Electrostatic boundary conditions for bilayer membranes	624
6.2. One curved (spherical or cylindrical) charged membrane	625
6.3. One undulating membrane	627
6.4. Membranes with variable surface charge density	628
7. A stack of charged lamellae	629
7.1. Suppression of Helfrich interactions by electrostatics	630
7.2. Rigidity of charged lamellae	633
8. Conclusions and future prospects	639
Acknowledgments	640
References	640

1. Introduction

Biological membranes are complex and heterogeneous objects separating living cells from their extra-cellular surroundings. Many of the membrane structural properties depend substantially on electrostatic interactions [1, 2], e.g., rigidity, structural stability, lateral phase transitions (the ‘main’ transition), and dynamics. Furthermore, electric charges have a very important role in processes involving more than one membrane such as membrane adhesion and cell-cell interaction, as well as the overall interaction of the membrane with other intra- and extra-cellular molecules.

The delicate interplay between charged membranes and their surrounding ionic solution can simply be explained as following. As any charged object immersed in an ionic solution, the membrane attracts a cloud of opposite charges forming a *diffusive* ‘electric double layer’ [1–5]. The exact distribution of the charges is given by the competition between the electrostatic interactions and the entropy of the ions in the solution which tends to disperse them. This diffusive electric double layer in turn influences the overall electrostatic interactions of the membrane with its environment as well as the ‘internal’ membrane properties.

Electrostatic interactions constitute a key component in understanding interactions *between* charged bodies in ionic solutions. For example, the stability of colloidal particles dispersed in a solvent [1, 2] can be explained by considering the competition between repulsive electrostatic interactions and attractive Van der Waals interactions. Electrostatic interactions are also of importance when considering interactions and adhesion between membranes. Furthermore, strong (unscreened) electrostatic interactions tend to rigidify flexible objects such as membranes and charged polymers (polyelectrolytes). Another characteristic of ions in solutions is that due to entropic effects, temperature is an important parameter controlling equilibrium properties.

The aim of this chapter is to review some of the basic considerations underlying the behavior of charged membranes in aqueous solutions. Due to the tremendous complexity of *real* biological membranes, we will restrict ourselves to very simple *model* charged membranes and will rely on the following assumptions and simplifications:

- We will mainly be concerned with the interplay between electrostatic interactions and the structure of the membrane *as a whole*. The membrane will be treated in the *continuum limit* as an interface with some degree of flexibility and with a given surface charge distribution. Equipotential membranes (of a given surface potential) will also be mentioned in some of the cases. We will not discuss special function regions within real heterogeneous membranes such as ion channels which have a specific biological function.
- This review will present in detail only theoretical results. Some experimental results will be mentioned. The reader should look at the chapter by Parsegian

and Rand for more details on experiments. The calculations are limited to solutions of the Poisson–Boltzmann equation (mean field theory). The finite size of the ions in the solution and within the membrane is ignored. The electric potential and the charge densities of the various ions are described by continuous variables (using the continuum hypothesis). For theoretical results which go beyond the continuum approach, we provide a few references and a short summary in the next section.

- We will not discuss the effect of electrostatics on dynamic properties of membranes and restrict ourselves to the static ones (in thermodynamical equilibrium) as well as fluctuations. These are the properties which are presently better understood. In addition, we will not consider the important interplay between electrostatics and other interactions (Van der Waals, hydration, etc.).

This review is organized in the following way: after some general considerations of charged surfaces in liquids and the derivation of the Poisson–Boltzmann equation (section 2), we present specific solutions of several electrostatic problems starting with a single flat and rigid membrane in section 3, and generalizing it to two flat membranes in section 4. Then, we consider the possibility of having a flexible membrane in various situations: a single membrane (section 6), two membranes, a stack of membranes, etc. (section 7). Special emphasis is given to the coupling between the electrostatic and the elastic properties. Some concluding remarks are presented in section 8.

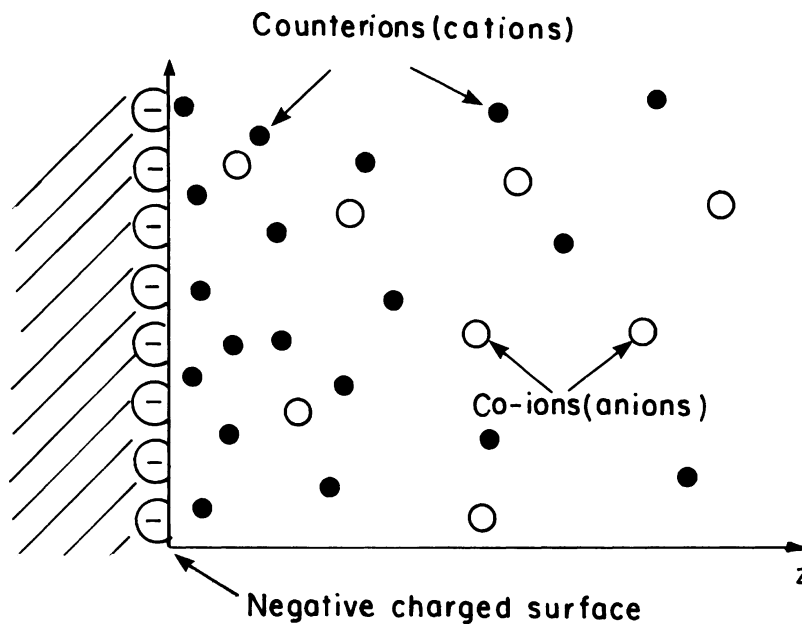


Fig. 1. Schematic illustration of the electric double layer problem. A surface which is negatively charged and immersed in an aqueous solution is attracting (positive) counterions and creates a depletion zone of the (negative) co-ions. The z axis denotes the distance from the surface. Adapted from ref. [2].

2. Charged surfaces in liquids: general considerations

Consider a charged and flat surface as displayed in fig. 1. In an ideal situation, this is a sharp boundary (located at $z = 0$) which limits the ionic solution to the half space $z > 0$. The ionic solution contains, in general, both anions and cations and is characterized by a dielectric constant ϵ_w assumed to be the dielectric constant of the water throughout the fluid. The boundary has two effects on the electrostatics of the system: (i) In the case of a charged boundary (equipotential boundary), the surface is characterized by a surface charge distribution (a surface potential). (ii) Even in the absence of surface charges, the boundary represents a discontinuous jump of the dielectric constant between the ionic solution and a different dielectric medium.

In fig. 2, a schematic view of a charged amphiphilic membrane is presented. The membrane of thickness t is composed of two monomolecular layers. The constituting molecules are amphiphiles having a charged moiety ('head') and an aliphatic moiety (hydrocarbon 'tail'). For phospholipid membranes, the molecules have a double tail (not drawn). We will model the membrane as a medium of thickness t having a dielectric constant ϵ_{oil} coming essentially from the closely packed hydrocarbon ('oily') tails. The molecular heads contribute to the surface charges and the entire membrane is immersed in an aqueous solution with a dielectric constant ϵ_w .

The surface charge can have two origins: Either a charge group (e.g., proton) dissociates from the polar head group into the aqueous solution leaving behind a charged surface, or an ion from the solution (e.g., Ca^{++}) binds to a neutral membrane. These processes are highly sensitive to the ionic strength and pH of the aqueous

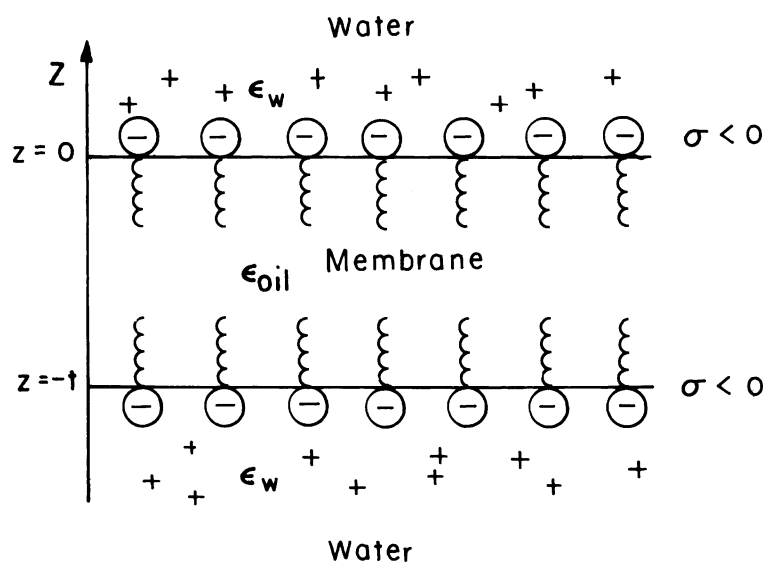


Fig. 2. A closer look at a bilayer membrane composed of two negatively charged surfaces, each of surface charge density σ . The membrane thickness is t and the 'inside' (hydrocarbon) dielectric constant is ϵ_{oil} . The water dielectric constant is $\epsilon_w \simeq 80$. The z axis denotes the distance from the membrane and its origin ($z = 0$) is chosen on the upper layer of the membrane.

solution. In many situations the finite thickness of the membrane can be safely taken to be zero and then the membrane surface is modeled like in fig. 1 – a single charged surface in contact with an ionic solution. We will see later in what conditions this frequently used limit is valid.

Without loss of generality, we assume that the membrane is negatively charged and take the surface charge density (per unit area) as a negative constant, $\sigma < 0$. In terms of the ionic solution itself, two different electrostatic situations will be distinguished throughout this review:

- (i) no electrolyte is added to the water, and the only ions in the solution are the counterions balancing exactly the charges within the membrane due to charge neutrality. Within the continuum hypothesis, the (positive) counterions in the solution at a point \vec{r} are described by a charge distribution $\rho_+(\vec{r}) = ez_+n_+(\vec{r})$, where the valency $z_+ = 1$ for monovalent ions, $e > 0$ is the electron unit charge and n_+ is the number density (per unit volume) of the counterions. Note, however, that even in pure water there is a finite concentration of H^+ and OH^- ions of about 10^{-7} M, due to a finite degree of dissociation of the water molecules themselves, making even pure water a very weak electrolyte.
- (ii) The solution is in contact with an electrolyte (salt) reservoir of fixed concentration n_0 . Two types of charge carries are present in the solution: co-ions and counterions and both types are in thermal equilibrium with the reservoir. We will not further differentiate between the activities of different ionic groups with the same charge. We assume for simplicity only one type of co-ions and one of counterions. The total charge density $\rho(\vec{r})$ at each point \vec{r} is the sum of the two ionic densities: $\rho(\vec{r}) = ez_+n_+(\vec{r}) + ez_-n_-(\vec{r})$, where z_+ (z_-) is the valency of the counterions (co-ions).

2.1. Poisson–Boltzmann equation

The relation between the electric potential $\psi(\vec{r})$ and the charge distribution $\rho(\vec{r})$ at any point \vec{r} is given by the Poisson equation

$$\nabla^2\psi = -\frac{4\pi}{\varepsilon_w}\rho(\vec{r}) = -\frac{4\pi e}{\varepsilon_w}(z_-n_- + z_+n_+) \quad (2.1)$$

where $\varepsilon_w \simeq 80$ is the dielectric constant of the aqueous solution taken as a constant within the fluid.

In principal, ψ and all other electrostatic properties can be evaluated for a given surface charge distribution (so-called Neumann boundary condition) or surface potential (so-called Dirichlet boundary condition). In this review we will mainly consider the Neumann boundary condition of fixed surface charge distribution, but it is rather straightforward to repeat the calculations for the constant surface potential case. (See also ref. [6] for another type of boundary condition where the degree of dissociation was allowed to be a variable chosen by the system.)

The Poisson equation (2.1) determines the electric potential for a given spatial charge distribution $\rho(\vec{r})$. However, even for a fixed *surface* charge distribution σ , the ions in the solution are mobile and can adjust their positions. In thermal equilibrium,

and using the continuum hypothesis, the ‘smeared out’ local density distributions of the two ions $n_{\pm}(\vec{r})$ (in units of number per unit volume) adjust to the presence of the electric potential. The electro-chemical potential μ_i of the i th ion is defined as $\mu_i = ez_i\psi + T \ln n_i$, where the first term is the electrostatic contribution and the second one comes from the (ideal) entropy of the ions in the weak solution limit. In thermal equilibrium μ_i remains constant throughout the system. Consequently, each ion density in the solution obeys a Boltzmann distribution according to the electric potential it feels:

$$n_i = n_0^{(i)} e^{-ez_i\psi/T}. \quad (2.2)$$

Note that we adopt the convention of expressing T in units of energy (setting the Boltzmann constant to unity). Combining eqs (2.1) and (2.2), we get the *Poisson–Boltzmann equation* which determines the potential ψ self-consistently

$$\nabla^2\psi(\vec{r}) = -\frac{4\pi e}{\epsilon_w} \left(z_+ n_0^{(+)} e^{-ez_+\psi(\vec{r})/T} + z_- n_0^{(-)} e^{-ez_-\psi(\vec{r})/T} \right). \quad (2.3)$$

Generally speaking, the Poisson–Boltzmann theory is a good approximation in most physiological conditions, especially for monovalent ions and for surface potentials which are not too large. Close to the charged surface, the finite size of the surface ionic groups and that of the counterions leads to deviations from the Poisson–Boltzmann results. In section 2.3 we mention a few results which are going beyond the Poisson–Boltzmann theory.

We discuss now separately the two electrostatic cases which were introduced in section 1. In the first case, no electrolyte is added, and the only ions in the solution are the counterions. Hence, $n_0^{(-)} = 0$ and we define $n_0 \equiv n_0^{(+)}$ as the reference density for which $\psi = 0$. The Poisson–Boltzmann equation (2.3) is then reduced to:

$$\nabla^2\psi(\vec{r}) = -\frac{4\pi en_0}{\epsilon_w} e^{-e\psi(\vec{r})/T}. \quad (2.4)$$

In the other situation where the system is in contact with a 1:1 electrolyte reservoir (e.g., Na^+Cl^-), $n_0^{(\pm)} = n_0$ is the electrolyte concentration in the reservoir and

$$\nabla^2\psi(\vec{r}) = \frac{8\pi en_0}{\epsilon_w} \sinh(e\psi(\vec{r})/T). \quad (2.5)$$

Note that although eq. (2.3) holds for any valencies z_{\pm} , in eqs (2.4)–(2.5) we inserted explicitly $z_{\pm} = \pm 1$. Only this case of monovalent ions will be discussed hereafter since it makes the mathematical derivation easier to follow. Divalent ions such as Ca^{++} have important consequences on the electrostatics of membranes [7]. Most of those consequences go beyond the continuum approach of the Poisson–Boltzmann theory.

Equations (2.4) and (2.5) are non-linear equations in the electric potential ψ . For some boundary conditions they can be solved analytically. However, in general, one

has to rely on numerical or perturbative solutions. Whereas the classical works in this field date from the beginning of the century with the works of Gouy [3] and Chapman [4] for the case of flat boundary conditions, application to flexible and charged membranes is a rather recent development.

A useful and quite tractable approximation to the full Poisson–Boltzmann equation (2.5) is its linearized version. This can be justified for surface potentials which are smaller than 25 mV at room temperature. Expanding the righthand side of eq. (2.5) to first order in ψ we get

$$\nabla^2 \psi(\vec{r}) = \lambda_D^{-2} \psi \quad (2.6)$$

where $\lambda_D = (8\pi n_0 e^2 / \epsilon_w T)^{-1/2} \sim n_0^{-1/2}$ is called the *Debye–Hückel screening length*. It varies from about 3 Å for a 1 M of 1:1 electrolyte like NaCl to about 1 μm for pure water (due to the ever presence of H⁺ and OH⁻ ions even in pure water with an ionic strength of about 10⁻⁷ M). In the presence of a relatively strong electrolyte, the electrostatic interactions are exponentially screened and can be effectively neglected for lengths larger than the Debye–Hückel screening length, λ_D . This is further explained in section 3.1.

2.2. Electrostatic free energy and electrostatic pressure

Up to now we discussed the Poisson–Boltzmann equation for the electric potential. It is also useful to evaluate the electrostatic *free energy* of the electric double layer problem as it will give us the electrostatic pressure between two charged surfaces in a liquid as well as the contribution to the membrane bending constant.

Two equivalent methods of calculating the electrostatic free energy are discussed at length by Verwey and Overbeek [1] leading to the following expression for the free energy per unit area

$$f_{\text{el}}[\sigma] = \int_0^\sigma \psi_s(\sigma') d\sigma' \quad (2.7)$$

where $\psi_s(\sigma')$ is the surface potential calculated for a fixed surface charge distribution σ' . The total free energy is obtained by integrating (2.7) over the entire charged surfaces. In the linear regime (eq. (2.6)), the free energy (2.7) simply reduces to $\frac{1}{2} \psi_s \sigma$ since the surface potential ψ_s is linear in the surface charge density σ .

Equation (2.7) can also be derived by considering the excess *bulk* free energy over that of the homogeneous electrolyte reservoir of concentration n_0 and with $\psi = 0$.

$$F_{\text{el}} = \frac{\epsilon_w}{8\pi} \int (\nabla \psi)^2 dV \quad (2.8)$$

$$+ T \int (n_+ \ln(n_+/n_0) + n_- \ln(n_-/n_0) - (n_+ + n_- - 2n_0)) dV$$

where the first term is the electrostatic internal energy, and the second accounts for the entropy of (monovalent) ions in the solution. Using the Poisson–Boltzmann equation and Green’s theorem, eq. (2.8) can be transformed into the surface integral, eq. (2.7). For the boundary condition of constant surface potential, a similar expression to (2.7) can be derived [8].

The electrostatic pressure can be calculated in several different ways [1, 2]. It is defined as the force per unit area felt by the two charged membranes (boundaries) separated by a distance d in the aqueous solution. One straightforward way of calculating the pressure $P(d)$ is to take the variation of the free energy with respect to the inter-membrane distance d : $P(d) = -\partial f_{\text{el}}/\partial d$. This is discussed in more detail in sections 4 and 7.

2.3. Beyond Poisson–Boltzmann: recent theory and experiment

As this review deals exclusively with the Poisson–Boltzmann theory, we mention here some recent theoretical results and experiments which go beyond the simpler Poisson–Boltzmann theory.

The assumptions which led to the derivation of the Poisson–Boltzmann equation (2.3) [3–5] can be summarized as follows: the ionic charge distributions are smeared out and are represented as smoothly varying functions. The discrete nature of the ions is not taken into account and no other molecular interaction between the ions and solvent molecules (water) is considered. See the chapters by Parsegian and Rand, Lipowsky, Helfrich and Evans in this Handbook and refs. [1, 2, 9–11] for a detailed discussion of Van der Waals, hydration and other forces occurring between surfaces in water.

Moreover, the Poisson–Boltzmann theory does not take into account any charge-charge correlations. Physical observables like the charge distributions are replaced by their thermal averages and, in this sense, resemble mean-field results. An extension of the Poisson–Boltzmann theory including effects of charge images and ion correlations has been developed for counterions (no-added electrolyte) [12] and for symmetric electrolytes [13]. At large separations the corrections to the Poisson–Boltzmann theory appear as an effective surface charge.

Another approach was used by Kjellander and Marcelja [14, 15]. The hard-core repulsion between ions for inhomogeneous Coulomb fluids with long range correlation has been formulated. This method relies on numerical solutions of the integral equations for the charge profiles between two boundaries using the *hypernetted chain* closure relation. In a more recent study [16] the hypernetted chain approach was compared with Monte Carlo simulations for 1:1, 1:2, and 2:2 electrolyte solutions. The agreement is good except for very short separation between the two boundaries.

Interesting behavior was observed for 2:1 electrolytes (e.g., Ca^{++}) [7] using the force machine apparatus to measure forces between charged surfaces immersed in aqueous calcium solutions. It was found that at small separation, the forces between the two surfaces can be attractive due to the presence of the calcium ions. This is in agreement with the anisotropic hypernetted chain calculations [7]. The consequences of those attractive forces at small separation on membrane adhesion are discussed in ref. [17]. See, for example, refs [14, 18, 19] for more details on recent experiments.

Finally, we mention an older attempt to improve upon the Poisson–Boltzmann theory close to the charge surface [1, 2, 20]. The Poisson–Boltzmann potential is used up to a distance δ from the surface. There, it is matched with a proximity potential which takes into account the finite size of the various ionic groups. This is the so-called *Stern* and *Helmholtz layer* effect and the thickness δ is of order one to two angstroms [21].

3. A single flat and charged membrane

The simplest problem to be solved using the Poisson–Boltzmann equation is for one *single-sided* flat membrane. The membrane surface occupies the $z = 0$ plane, and has a constant surface charge density σ (see figs. 1 and 2). The aqueous solution occupies the positive half space, $z > 0$. The electric field vanishes for large z , is taken as zero for $z < 0$, and is related to the surface charge density σ by the electrostatic boundary conditions at $z = 0$

$$\left. \frac{\partial \psi}{\partial z} \right|_{z=0} = -\frac{4\pi}{\epsilon_w} \sigma > 0. \quad (3.1)$$

The simplifying assumption that the electric field does not penetrate inside the ‘oily’ part of the membrane, namely, where the aliphatic ‘tails’ are packed, can be justified [22, 23] for typical values of membrane thickness and $\epsilon_{oil}/\epsilon_w$. It is valid as long as the ratio of the two dielectric constants, $\epsilon_{oil}/\epsilon_w$, is much smaller than the ratio t/λ_D , where t is the membrane thickness and λ_D is the Debye–Hückel screening length (see fig. 2). All our results for one and two *flat* membranes (sections 3–4) rely on this decoupled limit where the two sides (monolayers) of the membrane are completely decoupled and the electric field inside the membrane is zero. However, we will return to this point in a more quantitative way in section 6.

3.1. No added electrolyte

When no electrolyte is added, there is only one type of ions in the solution $n_+(z) = n(z)$ and the Poisson–Boltzmann equation (2.4) can be integrated exactly using the boundary condition (3.1). The potential and the counterion density distribution in the aqueous solution ($z > 0$) are given by

$$\begin{aligned} \psi(z) &= \frac{2T}{e} \ln(z + b) + \psi_0, \\ n(z) &= \frac{1}{2\pi l} \frac{1}{(z + b)^2}, \end{aligned} \quad (3.2)$$

where ψ_0 is a reference potential. Two useful lengths are introduced in eq. (3.2): the *Bjerrum length*, $l = e^2/(\epsilon_w T)$, and the so-called *Gouy–Chapman length*,

$$b = e/(2\pi|\sigma|l) = \epsilon_w T/(2\pi e|\sigma|).$$

Whereas the Bjerrum length is a constant length of about 7 Å for aqueous solutions at room temperature, the Gouy–Chapman length characterizes the thickness of the diffusive counterion layer close to the membrane (only when *no electrolyte is added* to the solution as in eq. (3.2)). Although the counterion profile decays slower than an exponential, the integrated amount of counterions (per unit area) attracted to the surface from $z = 0$ to $z = b$ is exactly $-\sigma/2$. Namely, it balances half of the surface charge. Note that the potential in eq. (3.2) has a logarithmic divergence at large z . This weak divergence is a consequence of the infinite lateral extent of the charged boundary (membrane) used to obtain eq. (3.2). The divergence will disappear for any membrane with finite dimensions.

3.2. Added electrolyte

In many biological situations, the charged membrane is in contact with a reservoir of electrolyte. Taking the bulk electrolyte concentration as n_0 , eq. (2.5) can be solved with the boundary condition (3.1) in addition to having a vanishing potential and electric field at infinity with $n_{\pm}(\infty) = n_0$. The resulting potential is

$$\psi(z) = -\frac{2T}{e} \ln \frac{1 + \gamma e^{-z/\lambda_D}}{1 - \gamma e^{-z/\lambda_D}} \quad (3.3)$$

where the parameter γ is the positive root of the quadratic equation:

$$\gamma^2 + \frac{2b}{\lambda_D} \cdot \gamma - 1 = 0. \quad (3.4)$$

The surface potential $\psi_s = \psi(0)$ is related to γ and hence to b/λ_D by

$$\psi_s = -\frac{4T}{e} \operatorname{arctanh}(\gamma). \quad (3.5)$$

Typical profiles of the potential $\psi(z)$ and the ion densities in the solution $n_{\pm}(z)$ are shown in fig. 3. Since the surface charge was taken as negative, one can see from eq. (3.1) that the potential tends to zero from below at large z . Hence, it is negative for all z values. At larger z , both densities n_{\pm} tend to the reservoir (bulk) value n_0 , where the potential is zero. However, their distributions are quite different close to $z = 0$ since the counterions are attracted to the charged surface whereas the co-ions are repelled from it.

In the limit of a strong electrolyte, the surface potential ψ_s is small enough so a linearization of the Poisson–Boltzmann equation can be justified. By either solving directly the linear Poisson–Boltzmann equation (2.6), or substituting the small ψ_s limit in eqs. (3.3)–(3.5) one obtains

$$\psi(z) = \psi_s e^{-z/\lambda_D} = -\frac{4\gamma T}{e} e^{-z/\lambda_D}. \quad (3.6)$$

One readily sees from (3.6) and fig. 3 that the electrostatic properties (e.g., electric potential, ionic concentration profiles) are strongly screened and decay exponentially in the Debye–Hückel limit of strong electrolytes. The ‘diffusive layer’ of ions in the solution is characterized by a ‘thickness’ λ_D . This thickness is quite different from the no-added electrolyte case, eq. (3.2). There, the algebraically decaying profile of counterions is characterized by the thickness b .

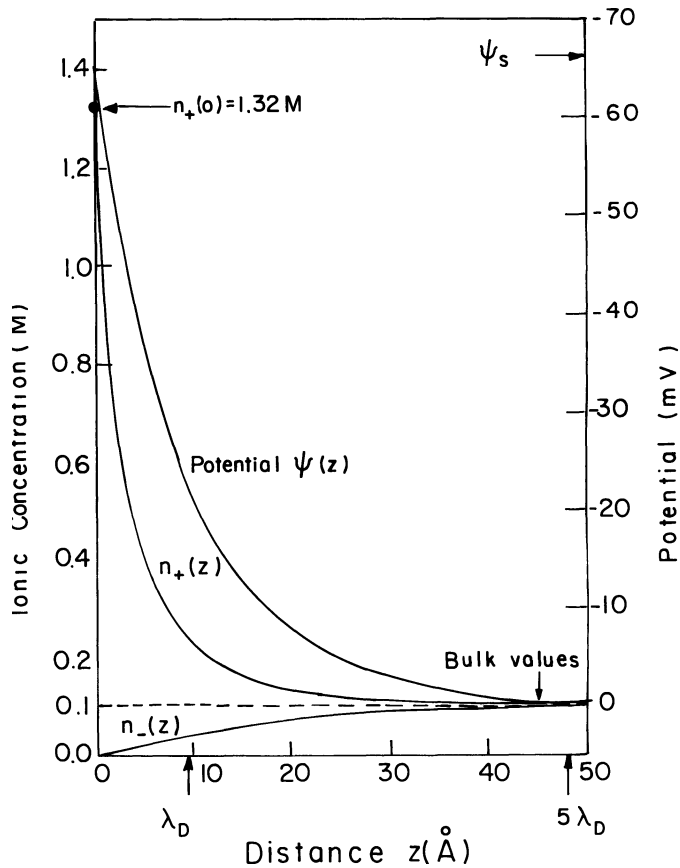


Fig. 3. Typical electric potential $\psi(z)$, counterion concentration $n_+(z)$ and co-ions concentration $n_-(z)$ profiles as function of the distance z from *one* charged surface. The electrolyte is monovalent with a bulk concentration of $n_0 = 0.1$ M. The surface charge is $\sigma = -0.0385$ electronic charge per \AA^2 , corresponding to about one charge per area of 26 \AA^2 and the surface potential is $\psi_s = -62.2$ mV. Distances corresponding to $\lambda_D \simeq 9.5 \text{ \AA}$ and $5\lambda_D \simeq 47.5 \text{ \AA}$ are denoted by arrows on the z axis. Adapted from ref. [2].

4. Two flat charged membranes

The results for a *single* flat membrane can be extended to include the case of *two* identically charged planar membranes [24] at a separation d , immersed in an aqueous solution as is illustrated in fig. 4. One membrane is located at $z = -d/2$ while the other is at $z = d/2$. The surface potential on both membranes is denoted by $\psi_s = \psi(z = \pm d/2)$, and the midplane one by $\psi_m = \psi(z = 0)$. Again two cases will be considered: (i) no electrolyte is added and the total amount of counterions in the solution exactly balances the surface charge. (ii) The aqueous solution is in contact with an electrolyte reservoir of concentration n_0 .

One of the interesting and measurable physical quantities is the electrostatic pres-

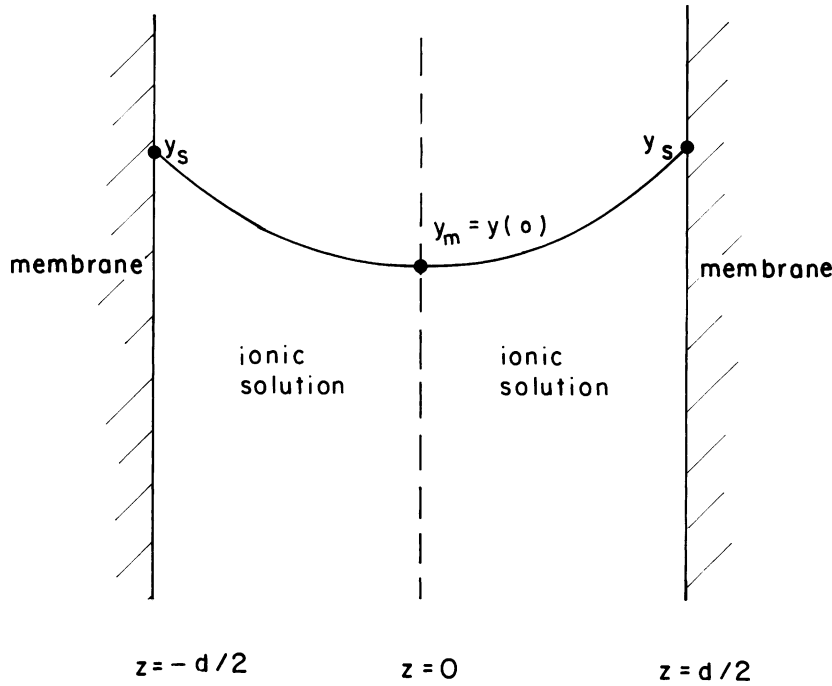


Fig. 4. Schematic drawing of a potential profile $y(z)$ (in rescaled units) between two membranes with the same negative charge separated by a distance d . The surface potential in rescaled units is $y_s = -e\psi_s/T$ and the midplane potential (where the electric field vanishes) is $y_m = -e\psi_m/T$.

sure P felt by the membranes. It is equal (up to a sign) to the variation of the free energy density with respect to the inter-membrane distance d , eq. (2.7), $P(d) = -\partial f_{el}/\partial d$. For two *flat* boundaries, it can be shown [1, 2] that P is directly proportional to the increase in the concentration of ions at the midplane. Namely, $P(d)$ is the excess in osmotic pressure of the ions at the midplane over the bulk pressure

$$P(d) = T \sum_{i=\pm 1} (n_i(z=0) - n_0^{(i)}) \quad (4.1)$$

where $\sum_i n_i(z=0)$ is the total ionic concentration at the midplane and $\sum_i n_0^{(i)}$ is known from the electrolyte reservoir concentration.

4.1. No added electrolyte

In this case the Poisson–Boltzmann equation (2.4) can be solved analytically [2, 25, 26]. Since the two boundaries at $z = \pm d/2$ are symmetric about $z = 0$ (fig. 4), it is sufficient to solve the Poisson–Boltzmann equation only in the interval $[0, d/2]$. The appropriate boundary conditions are $\partial\psi/\partial z|_{z=d/2} = (4\pi/\epsilon_w)\sigma < 0$ on the membrane;

and from symmetry, a vanishing electric field at the midplane: $\partial\psi/\partial z|_{z=0} = 0$. Combining these boundary conditions with the differential equation, eq. (2.4), results in analytical expressions for $\psi(z)$ and $n(z)$:

$$\begin{aligned}\psi(z) &= \frac{T}{e} \ln(\cos^2 Kz) < 0, \\ n(z) &= n_m e^{-e\psi(z)/T} = \frac{n_m}{\cos^2 Kz}.\end{aligned}\quad (4.2)$$

Note that the midplane potential ψ_m is taken as the reference potential, and $n_m = n(z=0)$ is the midplane ionic concentration. The length K^{-1} (to be distinguished from the Debye–Hückel screening length λ_D) is related to n_m via

$$K^2 = \frac{2\pi e^2}{\varepsilon_w T} n_m \quad (4.3)$$

and in turn can be related to the surface charge density σ using the membrane boundary condition

$$Kd \tan(Kd/2) = -\frac{2\pi e\sigma}{\varepsilon_w T} d = \frac{d}{b} \quad (4.4)$$

where the Gouy–Chapman length $b = -\varepsilon_w T / (2\pi e\sigma) \sim \sigma^{-1}$ was defined already after eq. (3.2).

The pressure (4.1) in the case of no-added electrolyte [25, 26] is simply $P(d) = Tn_m$ or in terms of K from eq. (4.3)

$$P(d) = \frac{\varepsilon_w T^2}{2\pi e^2} K^2 = \frac{T}{2\pi l} K^2. \quad (4.5)$$

Two limits can now be discussed depending on the ratio d/b in eq. (4.4): (i) small surface charge density, $d/b \ll 1$, called the ideal-gas regime; and (ii) large surface charge density, $d/b \gg 1$, called the Gouy–Chapman regime. These two limits will be discussed in more detail in the next section when we consider the added electrolyte case. The former case, $d/b \ll 1$, yields from (4.4) $Kd \ll 1$ and $K^2 = 2/(bd)$. This is the case where the variation of the potential profile and ion concentration between the plates is minimal. The pressure varies like $1/d$, and essentially comes from the entropy of a homogeneous *ideal gas* of ions in solution

$$P(d) = -\frac{T}{d} \frac{2\sigma}{e} = \frac{T}{\pi l b} \frac{1}{d} \quad (4.6)$$

since $-2\sigma/ed$ is the average density of counterions needed to neutralize the two surfaces of surface charge σ each.

In the other limit of large surface charge density $d/b \gg 1$, one can see from eq. (4.4) that $Kd/2$ approaches a limiting value of $\pi/2$. The pressure varies as $1/d^2$

$$P(d) = \frac{\pi T}{2l} \frac{1}{d^2} = \frac{\pi \varepsilon_w T^2}{2e^2} \frac{1}{d^2} \quad (4.7)$$

and is independent of the surface charge density σ . The last equation is closely related to the *Langmuir equation* [27] which describes the electrostatic contribution to the disjoining pressure of wetting films. This is the region where the electrostatic interactions are long range and unscreened. Of course, even in pure water the effective Debye–Hückel screening length is about $1 \mu\text{m}$ and the electrostatic interactions will always be screened for larger distances.

The electrostatic free energy can be evaluated either directly from (2.7) or as the integral over the pressure: $f(d) - f_\infty = \int P(d) \delta d$. In the ideal-gas limit ($b \gg d$) it varies as $\ln d$, whereas in the strong surface charge limit ($b \ll d$) it varies as $1/d$.

We turn now to the added electrolyte case. Note that the no-added electrolyte case discussed above can be obtained formally as the limit of vanishing electrolyte strength (very large λ_D). This will be shown in the next section.

4.2. Added electrolyte

When an aqueous solution between the two membranes is in contact with an electrolyte reservoir, the appropriate Poisson–Boltzmann equation to solve is eq. (2.5) as was explained in section 2. For a single membrane, the potential can be evaluated analytically as in eq. (3.3). However, for two charged membranes, ψ can only be expressed as an elliptic integral [1].

In terms of a dimensionless potential $y(z) \equiv -e\psi(z)/T$, eq. (2.5) and the boundary conditions are written as

$$\begin{aligned} \frac{\partial^2 y}{\partial z^2} &= \lambda_D^{-2} \sinh y, \\ \frac{\partial y}{\partial z} \Big|_{z=d/2} &= \frac{2}{b}, \quad \frac{\partial y}{\partial z} \Big|_{z=0} = 0. \end{aligned} \quad (4.8)$$

Using the notation $y_s \equiv y(d/2)$ on the membrane and $y_m \equiv y(0)$ on the midplane (see fig. 4) the first integration of eq. (4.8) yields

$$\lambda_D \frac{\partial y}{\partial z} = \sqrt{2 \cosh y(z) - 2 \cosh y_m}. \quad (4.9)$$

Note that $y(z) > 0$ (since it is proportional to $-\psi(z)$) for the entire interval $[0, d/2]$ and $y_s > y_m > 0$. A second integration of eq. (4.9) results in an elliptic integral which determines the potential y at any point of space z

$$z = \lambda_D \int_{y_m}^y (2 \cosh y' - 2 \cosh y_m)^{-1/2} dy'. \quad (4.10)$$

The boundary condition (4.8) combined with eq. (4.9) gives one relation between y_m and y_s

$$\frac{2}{b^2} \lambda_D^2 = \cosh y_s - \cosh y_m \quad (4.11)$$

whereas a second relation is obtained by substituting $z = d/2$ in eq. (4.10). Thus, up to performing the elliptical integration in (4.10), the profile $y(z)$ is uniquely determined and depends only on the three parameters in our problem: the spacing d , the surface charge σ and the reservoir concentration n_0 .

The general expression for the pressure $P(d)$ is obtained from (4.1) where the midplane ionic concentration for each charge is $n_m^{(\pm)} = n^{(\pm)}|_{z=0} = n_0 \exp(\pm y_m)$. Then

$$P(d) = T(n_m^{(-)} + n_m^{(+)} - 2n_0) = 2Tn_0(\cosh y_m - 1). \quad (4.12)$$

Since the elliptical integral in (4.10) can be solved only numerically, it is useful to separate the general solution of eq. (4.10) into several limits where approximate potentials and free energies can be calculated analytically. We will define these limits in terms of the three introduced lengths: the spacing between the two membranes d , the Debye–Hückel screening length $\lambda_D \sim n_0^{-1/2}$, and the Gouy–Chapman length $b \sim \sigma^{-1}$. As can be seen from fig. 5, the parameter space $(b/d, \lambda_D/d)$ is divided into four regions: the ideal-gas region; the Gouy–Chapman region; the Intermediate region and the Debye–Hückel region. The ideal-gas and Gouy–Chapman regions are limiting cases of no-added electrolyte (discussed in section 4.1) as will be demonstrated below.

4.2.1. Ideal-gas region

The elliptic integral (4.10) can be evaluated in the limit of large potential $y(z) \gg 1$ ($|e\psi(z)| \gg T$) and small membrane separation $d \ll \lambda_D$. Substituting $z = d/2$ in eq. (4.10) yields a relation between y_s and y_m :

$$e^{-(y_s - y_m)/2} = \cos\left(\frac{d}{4\lambda_D} e^{y_m/2}\right). \quad (4.13)$$

Another relation between y_s and y_m is obtained from the boundary condition (4.11) in the same limit of large $y(z)$

$$\frac{4\lambda_D^2}{b^2} = e^{y_s} - e^{y_m}. \quad (4.14)$$

The above expressions for y_m and y_s hold for both the ideal-gas and Gouy–Chapman regions of fig. 5 where the separation d is small and the potential is large. The difference between the two regions is that $\lambda_D^{-1} d \exp(y_m/2) \ll 1$ for the ideal-gas case, whereas for the Gouy–Chapman case $\lambda_D^{-1} d \exp(y_m/2) \simeq \pi$. Identifying $\lambda_D^{-1} \exp(y_m/2)$ with K of section 4.1 (no added electrolyte), we recover the no-added electrolyte limit of large λ_D .

The pressure for the ideal-gas region is just $P(d) = Tn_0 \exp(y_m)$ using the large y_m limit of (4.12). From eqs (4.12)–(4.14) one obtains

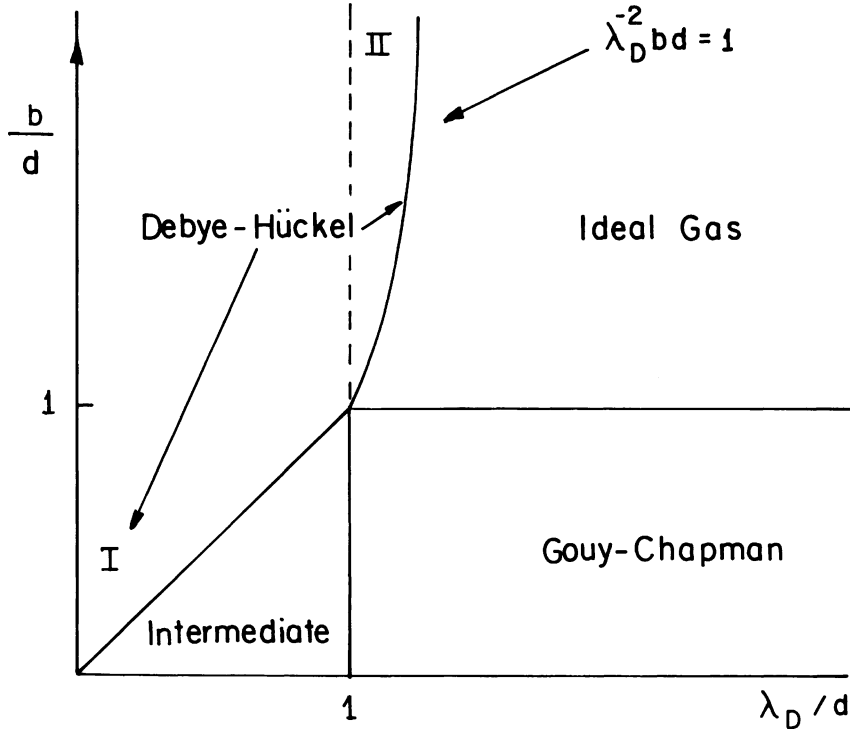


Fig. 5. Schematic representation of various limits of the full Poisson–Boltzmann equation for two flat charged surfaces. The diagram is plotted in terms of two dimensionless ratios: b/d and λ_D/d where b is the Gouy–Chapman length (appeared first in eq. (3.2)), d is the inter-membrane spacing and λ_D is the Debye–Hückel screening length. The four regions discussed in the text are: the linear Debye–Hückel regime, the ideal-gas regime, the Gouy–Chapman regime and the Intermediate regime. Apart from the line $\lambda_D^{-2} b d = 1$ separating the ideal-gas and Debye–Hückel regions, all crossover loci are straight lines. At those lines, the limiting solutions both for the potential $\psi(z)$ and the pressure $P(d)$ crossover smoothly from one regime to another. This diagram also applies to the different regimes used in section 7 in calculating the electrostatic contribution to the bending modulus, $\delta\kappa^e$, with one exception. Namely, the Debye–Hückel region is divided in two: the large-spacing Debye–Hückel (marked as region I) and the small-spacing one (marked as region II). Adapted from ref. [60].

$$P(d) = -\frac{2T\sigma}{e} \frac{1}{d} = \frac{T}{\pi l b} \frac{1}{d},$$

$$f_{el} = \frac{2T\sigma}{e} \ln d = -\frac{T}{\pi l b} \ln d.$$
(4.15)

The above expression coincides exactly with the no-added electrolyte limit, eq. (4.6), in the same limit of weak surface charges, and is independent of the Debye–Hückel screening length, λ_D . The limits of validity of the ideal-gas region are, hence,

$\lambda_D \gg d$; $y_m, y_s \gg 1$; and $d \exp(y_m/2) \ll \lambda_D$. In fig. 5 they correspond to the region

$$b/d \gg 1 \quad \text{and} \quad (\lambda_D/d)^2 \gg b/d. \quad (4.16)$$

As both the surface charge density and the electrolyte strength are small in the ideal-gas region, the main contribution to the electrostatic pressure comes just from the entropy of mixing of the ions and not from their charges. The potential as well as the ionic density are almost constant throughout the region between the membranes.

4.2.2. Gouy–Chapman region

Repeating the above calculation for the limit $\lambda_D^{-1} d \exp(y_m/2) \simeq \pi$; $\lambda_D \gg d$, and $y_s \gg y_m \gg 1$, yields a different limiting value of the pressure. This is the limit of a strong surface charge density and weak electrolyte. It coincides exactly with the previous obtained results for the Gouy–Chapman regime (strong charges) for the no-added electrolyte case, eq. (4.7)

$$P(d) = \frac{\pi T}{2l} \frac{1}{d^2}, \quad (4.17)$$

$$f_{\text{el}} = \frac{\pi T}{2l} \frac{1}{d} = \frac{\pi \varepsilon_w T^2}{2e^2} \frac{1}{d}.$$

In the Gouy–Chapman region the electrostatic interactions are the strongest and the least screened. In fig. 5, the limits of validity for this region are shown as

$$b/d \ll 1 \quad \text{and} \quad \lambda_D/d \gg 1. \quad (4.18)$$

4.2.3. Intermediate region

When the separation between the membranes is large compared to λ_D , the potential at the midplane is always small, $y_m \ll 1$, and the coupling between the two membranes is weak even when the surface potential y_s on each surface is large. Thus, y_m is obtained by a linear superposition of the midplane potentials of two *non-interacting* membranes. Using the previously obtained potential for a single flat membrane, eq. (3.3), yields

$$y_m = 8\gamma e^{-d/2\lambda_D} \quad \text{and} \quad \gamma = \tanh(y_s/4) \approx 1. \quad (4.19)$$

The pressure expression (4.12) can be linearized since y_m is small, leading to

$$P(d) = T n_0 y_m^2 = 64\gamma^2 T n_0 e^{-d/\lambda_D}. \quad (4.20)$$

Since $\gamma \approx 1$ and $\lambda_D^2 = 1/(8\pi n_0 l)$, the pressure for the Intermediate region can be expressed as

$$P(d) = \frac{8T}{\pi l \lambda_D^2} e^{-d/\lambda_D}, \quad (4.21)$$

$$f_{\text{el}} = \frac{8T}{\pi l \lambda_D} e^{-d/\lambda_D} = \frac{8\varepsilon_w T^2}{\pi e^2 \lambda_D} e^{-d/\lambda_D}.$$

Since the distance between the two membranes is large ($d \gg \lambda_D$), the interaction and the exerted pressure on the membranes fall off exponentially with the inter-membrane distance d . Note that unlike the expression for the pressure, the Poisson–Boltzmann equation itself *cannot* be linearized since the surface potential y_s is large.

The limits of validity of this region are (see fig. 5)

$$\lambda_D \gg b \quad \text{and} \quad \lambda_D/d \ll 1. \quad (4.22)$$

4.2.4. Debye–Hückel region

When the potential value on the membrane surface is small (less than 25 mV at room temperature), the Poisson–Boltzmann equation can be linearized. This is the Debye–Hückel region. Solving the linear equation for the two membrane problem, we get

$$\begin{cases} y_s = \frac{2\lambda_D}{b} \coth(d/2\lambda_D), \\ y_m = \frac{y_s}{\cosh(d/2\lambda_D)}. \end{cases} \quad (4.23)$$

As in the Intermediate region, the pressure and the free energy excess depend linearly on y_m yielding

$$P(d) = \frac{T}{2\pi l b^2} \frac{1}{\sinh^2(d/2\lambda_D)}, \quad (4.24)$$

$$f_{el} = \frac{T\lambda_D}{\pi l b^2} (\coth(d/2\lambda_D) - 1) = \frac{4\pi\sigma^2\lambda_D}{\varepsilon_w} (\coth(d/2\lambda_D) - 1).$$

Note that the limits of validity of the Debye–Hückel region extend all the way from large inter-membrane spacing and weak overlap ($\lambda_D/d \ll 1$ denoted as region I on fig. 5) to small spacing and strong overlap ($\lambda_D/d \gg 1$ denoted as region II on fig. 5). For small d (region II), the Debye–Hückel region satisfies the conditions

$$(\lambda_D/d)^2 \ll b/d \quad \text{and} \quad \lambda_D/d \gg 1 \quad (4.25)$$

and the line $b/d \simeq (\lambda_D/d)^2$ indicates the crossover into the ideal-gas region. On the other hand, for large d (region I) the Debye–Hückel region crosses over into the Intermediate region on the line $\lambda_D \simeq b$. The Debye–Hückel region there is valid for

$$\lambda_D \ll b \quad \text{and} \quad \lambda_D/d \ll 1. \quad (4.26)$$

We remark that the crossover lines are not lines of singularities. They are rather lines where the expressions for the pressure $P(d)$ and potential profiles $\psi(z)$ crossover smoothly from one regime to another. The agreement between those approximations

and the exact numerical integration of the full Poisson–Boltzmann equation is rather satisfactory [28].

This concludes our discussion on the electric double layer problem of *flat* membranes. As was mentioned in section 1, the profiles $\psi(z)$ and $n(z)$ as well as the electrostatic free energy and pressure are used extensively in analyzing experimental data of charged membranes. For monovalent ions, the Poisson–Boltzmann theory agrees quite well with experiments. Even within the simplifying approximations used in this review, we presented a few electrostatic regimes with different behavior for planar and rigid membranes. In the remainder of this review we will consider an even more complicated situation where the membranes are allowed to have some flexibility and curvature.

5. Flexible and charged membranes: general considerations

In many cases, amphiphilic membranes (as opposed to polymerized membranes) have a certain amount of ‘fluidity’. The fluidity depends crucially on the temperature as well as on other system parameters. Fluid membranes can be thought of as interfaces with a liquid-like response to inplane shear and elastic response to out-of-plane deformation [29, 30]. For many biological systems the elastic constants characteristic of the bending modes, vary between few dozens T (rigid membranes) to as low as one T (very flexible membranes).

When the membranes are flexible, they can be easily deformed and will have structural changes due to thermal fluctuations. The entire electrostatic problem for flat and rigid membranes, as was done in the previous sections, has to be reformulated in order to apply to more complicated geometries. Other examples of inherent deviations of membrane shapes from flat geometries are ‘rippled’ phases ($P_{\beta'}$) of lipid membranes where the ripples are believed to be equilibrium structures resulting from various competing membrane interactions [31–36].

Understanding the delicate coupling between the electric double layer problem and membrane shape, deformation and instabilities has been an active field of research in recent years. However, this problem turned out to be extremely complex. The main difficulty is related to solving the full (non-linear) Poisson–Boltzmann equation together with complicated electric boundary conditions. A further complication is the effect of the charges on the boundary conditions themselves. Unlike solid objects with fixed charge distributions, the membrane shape can adjust to some degree in response to external forces such as the electric field. Thus, the membrane shape and electrostatics are coupled and need to be considered together.

Similar problems of comparable difficulty arise in the theory of polyelectrolytes [37, 38] – charged flexible polymers in aqueous solutions – as well as charged ‘worm-like’ cylindrical micelles [38, 39]. In these cases the shape conformation, stiffness and electrostatics are intimately related. The statistics of the polyelectrolyte chains depends on the local electric field and counterion distribution, which in turn depend on the polyelectrolyte chain configuration.

Lacking a global picture of the interplay between electrostatics and membrane shape, we will review in the following theoretical results which address only specific

aspects of the coupling between electrostatic and structural properties as reflected in the membrane elastic constants. We will explain the interplay between electrostatics and entropically induced repulsive forces (the so-called Helfrich interactions [40]), but will neglect, for simplicity, all other inter-membrane interactions like hydration and Van der Waals interactions.

6. A single charged and flexible membrane

How do the charges affect the elastic properties of fluid-like membranes? To address this issue let us first mention the continuum model for the elastic energy of fluid-like membranes. This model was proposed by Helfrich in analogy to *smectic* phases of liquid crystals [29]. The phenomenological elastic energy is expressed as an integral over the membrane area

$$f_{\text{bend}} = \frac{1}{2} \kappa \int (c_1 + c_2 - c_0)^2 dS + \kappa_G \int c_1 c_2 dS \quad (6.1)$$

where κ and κ_G are the mean and Gaussian elastic moduli, respectively. The two principal curvatures are c_1 and c_2 whereas c_0 is the *spontaneous curvature*. For a single amphiphilic layer c_0 expresses the internal tendency of the layer to curve towards the water, $c_0 > 0$, or away from the water, $c_0 < 0$. The tendency to curve is a result of the different molecular structure and interactions of the head and tail moieties of the amphiphiles. For bilayer membranes composed of two identical layers $c_0 = 0$ from symmetry reasons. But c_0 can be non-zero if the composition of the two layers of the membrane differs. The membrane also is assumed to be incompressible. Hence, all the contributions to the surface tension (including those arising from electrostatics) vanish [41, 42].

The electrostatic contribution to κ and to κ_G are denoted, respectively, as $\delta\kappa^{\text{el}}$ and $\delta\kappa_G^{\text{el}}$. It has been calculated for a variety of geometries: cylinders, spheres and sinusoidal undulating membranes. The electrostatic contribution to the bending moduli can be identified by expanding the electrostatic free energy up to second order in the local curvatures c_1 and c_2 , and comparing the expansion with the elastic energy per unit area, eq. (6.1), of the same object: a sphere of radius R , a cylinder of radius R , or an sinusoidal undulating membrane with wavelength $2\pi/q$ and amplitude u

$$\begin{aligned} f_{\text{bend}} &= \frac{1}{2} \kappa \left(\frac{2}{R} - c_0 \right)^2 + \kappa_G \left(\frac{1}{R} \right)^2, & \text{sphere,} \\ f_{\text{bend}} &= \frac{1}{2} \kappa \left(\frac{1}{R} - c_0 \right)^2, & \text{cylinder,} \\ f_{\text{bend}} &= \frac{1}{4} \kappa q^4 u^2, & \text{sinusoidal undulation } (c_0 = 0). \end{aligned} \quad (6.2)$$

Before presenting the electrostatic contributions to the bending moduli, we would like to explain the different ways the electrostatic boundary conditions can be formulated as one considers a *bilayer* membrane of finite thickness t . Namely, in what way are the two sides of the bilayer coupled electrically.

6.1. Electrostatic boundary conditions for bilayer membranes

Is the finite thickness of the membrane (denoted t in figs 2 and 6) of importance for the electrostatics properties of the membrane? Can one safely take the limit of membrane thickness to zero? Those questions have already arose in sections 3 and 4 for flat bilayer membranes. The answer is that there are two limiting behaviors as the thickness of the membrane becomes very small. The first is a limit of a bilayer which is composed of two (electrically) *completely decoupled* monolayers. In this case no electric energy is stored inside the membrane. This limit is sometimes called the ‘opaque’ or ‘adsorbing’ limit [43]. It corresponds to a vanishing membrane thickness t but with $t/\lambda_D \gg \epsilon_{oil}/\epsilon_w$ (figs 2 and 6). For this decoupled limit, $\delta\kappa^{el}$ of the bilayer is equal to twice the contribution of a single monolayer. When the ratio $\epsilon_{oil}/\epsilon_w$ is small, e.g., as in physiological conditions where this ratio is about 1/40, this limit is quite reasonable and it is used quite often in calculations. This is also the limit used throughout sections 3 and 4 for flat membranes. The other limit of $t/\lambda_D \ll \epsilon_{oil}/\epsilon_w$ (sometimes called the ‘transparent’ limit [43]) occurs when the two monolayers are *completely coupled* electrically. It is further discussed in refs [44, 45].

It is also possible to address the full (albeit more difficult) problem [22, 45] of an arbitrary electrostatic coupling between the two sides of the membrane. It is useful then to define the parameter $s \equiv (\lambda_D/t)(\epsilon_{oil}/\epsilon_w)$ and to consider its range of possible values. For typical values of water and oil dielectric constants, $\epsilon_w = 80$ and $\epsilon_{oil} \simeq 2$,

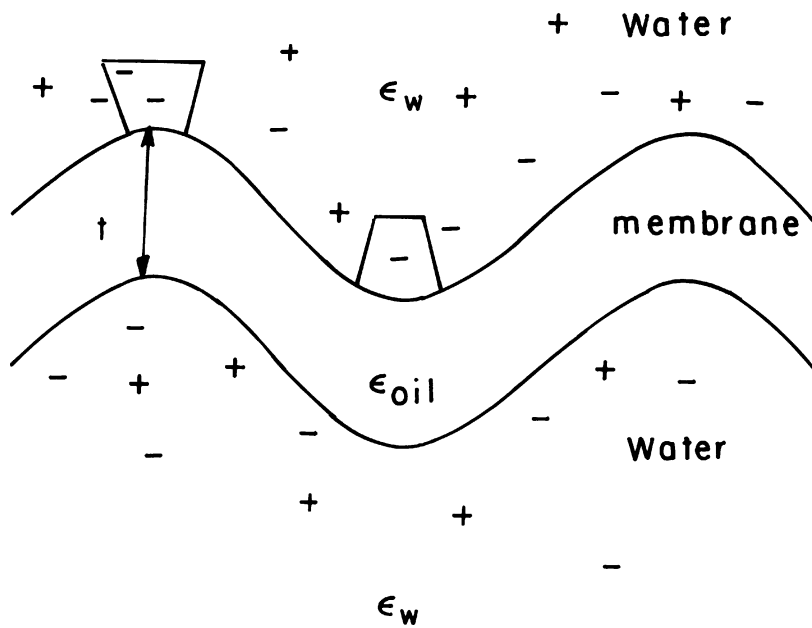


Fig. 6. A bilayer membrane of thickness t and surface charge density σ as in fig. 2 but here the flexible membrane is undulating in an aqueous solution. Notice the larger volume per unit surface area, accessible to the ions in the solution, in the convex parts as compared with to the concave parts.

we get $s \simeq \lambda_D/(40t)$. The small and large s limits correspond, respectively, to the fully decoupled and coupled limits introduced above.

Another possible boundary condition is to take the membrane as a surface of an electric conductor. The membrane is characterized by a fixed surface potential (Dirichlet boundary conditions). This different electrostatic problem was treated separately in some works [8, 43, 44]. However, most of the results we will present are for the fixed surface charge densities.

We note that ‘real’ membranes do not satisfy any of those boundary conditions exactly. In a real membrane the charges are not frozen as on a perfect insulator, since they have an inplane mobility. In addition they can dissociate with different rates from different regions of the membrane. These two factors contribute to the redistribution of charges within the membrane. However, the membrane is not an equipotential surface either (like a metallic conductor). The motivation of studying those model systems with simplified electrostatic boundary conditions is that hopefully one can elucidate the more complex behavior of biological membranes.

6.2. One curved (spherical or cylindrical) charged membrane

6.2.1. Debye–Hückel limit of one decoupled bilayer

Winterhalter and Helfrich [46] calculated the free energy, eq. (2.7), of a single charged cylindrical membrane by solving the Poisson–Boltzmann equation in cylindrical coordinates. The calculation was also repeated for a sphere. They treated only the linearized Poisson–Boltzmann equation (strong electrolytes). Expanding the electrostatic free energy to order $1/R^2$, the electrostatic contribution to the bending modulus $\delta\kappa^{\text{el}}$ per each monolayer of the bilayer membrane is obtained

$$\begin{aligned}\delta\kappa^{\text{el}} &= \frac{3\pi}{2} \frac{\sigma^2 \lambda_D^3}{\varepsilon_w} = \frac{3T}{8\pi l} \frac{\lambda_D^3}{b^2}, \\ \delta\kappa_G^{\text{el}} &= -\frac{\pi\sigma^2 \lambda_D^3}{\varepsilon_w} (1 + \lambda_D^{-1}t).\end{aligned}\tag{6.3}$$

Note that in some works, $\delta\kappa^{\text{el}}$ is defined *per bilayer* which gives an extra factor of two. The above result are obtained in the decoupled limit of the bilayer (zero s). Since the results are obtained for a *single* bilayer, they correspond to taking *first* the limit of large inter-membrane separation d and then looking at region I (close to the origin) of the Debye–Hückel regime in fig. 5, where $b/\lambda_D \gg 1$ and $d/\lambda_D \gg 1$. As is apparent from eq. (6.3), electrostatics stiffen the membrane since $\delta\kappa^{\text{el}} > 0$. The other effect is a negative contribution to κ_G which will make saddle points less favorable. As long as $2\kappa + \kappa_G > 0$, the flat membrane is stable with respect to shape fluctuations. Hence, the electrostatic contribution, eq. (6.3), tends to stabilize the flat membrane, but the overall stability of the membrane depends also on the contribution to κ and κ_G coming from the aliphatic tails of the amphiphiles. We remark that in some more special situations (discussed below), the electrostatic contribution to the bending moduli can destabilize a flat membrane, which then transforms into, e.g., a vesicle [46].

6.2.2. Debye–Hückel limit: generalization to one coupled bilayer

Kiometzis and Kleinert [22] generalized the results of Winterhalter and Helfrich [46] for the decoupled limit. They considered the more general case of a coupled bilayer with any value of $s = (\lambda_D/t)(\varepsilon_{\text{oil}}/\varepsilon_w)$ (see figs. 2 and 6), while still working in the linear Debye–Hückel limit of the Poisson–Boltzmann equation for a single bilayer of thickness t . Here, the electric field is not zero inside the membrane but satisfies the two boundary conditions on the two sides of the membrane. Their result for the bending moduli read

$$\begin{aligned}\delta\kappa^{\text{el}} &= \frac{\pi\sigma^2\lambda_D^3}{2\varepsilon_w} \left(1 + \frac{2}{1+2s}\right), \\ \delta\kappa_G^{\text{el}} &= -\frac{\pi\sigma^2\lambda_D^3}{\varepsilon_w} \left(1 + \lambda_D^{-1}t - \frac{1}{2}(\lambda_D^{-1}t)^2\right).\end{aligned}\tag{6.4}$$

Note that eq. (6.3) is recovered in the limit of zero s (the decoupled limit), whereas the other limit of completely coupled bilayer (large s) leads to a reduction of $\delta\kappa^{\text{el}}$ by a factor of three. On the other hand, the value of $\delta\kappa_G^{\text{el}}$ stays the same as it is independent of s .

6.2.3. Intermediate regime: weak electrolyte

Lekkerkerker [47] and Ninham and Mitchell [48] extended the linear Poisson–Boltzmann results (strong electrolyte) to the general electrolyte case. They solved the non-linear Poisson–Boltzmann equation for a single charged cylinder or sphere immersed in an electrolyte. It is convenient to express the Poisson–Boltzmann equation in cylindrical or spherical coordinates:

$$\begin{aligned}\nabla^2 y &= \frac{d^2 y}{dr^2} + \frac{1}{r} \frac{dy}{dr} = \lambda_D^{-2} \sinh y \quad (\text{cylindrical coordinates}), \\ \nabla^2 y &= \frac{d^2 y}{dr^2} + \frac{2}{r} \frac{dy}{dr} = \lambda_D^{-2} \sinh y \quad (\text{spherical coordinates}).\end{aligned}\tag{6.5}$$

The contribution to the bending moduli was calculated from the electrostatic free energy in the completely decoupled limit (zero s). For simplicity, we quote here only their results in the limit of a weak electrolyte and high surface charge density corresponding to the Intermediate region of fig. 5, $b \ll \lambda_D$ and $\lambda_D/d \ll 1$. More details can be found in refs [47, 48].

$$\begin{aligned}\delta\kappa^{\text{el}} &= \frac{\varepsilon_w \lambda_D}{2\pi} \left(\frac{T}{e}\right)^2 = \frac{T}{2\pi l} \lambda_D, \\ \delta\kappa_G^{\text{el}} &= -\frac{\pi\varepsilon_w \lambda_D}{6} \left(\frac{T}{e}\right)^2 = -\frac{\pi T}{6l} \lambda_D.\end{aligned}\tag{6.6}$$

Taking $\sigma = 0.15$ Coulomb per m^{-2} (about one charge per typical amphiphile compact area) and electrolyte strength of 0.4 M to 0.01 M, $\delta\kappa^{\text{el}}$ and $\delta\kappa_{\text{G}}^{\text{el}}$ vary from about 0.1 T to 1 T . Hence, electrostatic interactions have a significant effect on the elastic properties only if the uncharged (bare) membrane is flexible enough with bending moduli of order of T . In experiments, such flexible membranes have been realized by introducing a co-surfactant (short chain alcohol) which reduces substantially the ‘tail’ part of the bending moduli [49, 50]. Checking the overall electrostatic contribution to the bending (for zero spontaneous curvature, $c_0 = 0$), one can see from (6.6) that $2\delta\kappa^{\text{el}} + \delta\kappa_{\text{G}}^{\text{el}} < 0$. Hence, electrostatic interactions will tend to destabilize a flat membrane in this unscreened limit.

6.3. One undulating membrane

Results for electrostatic corrections to the bending moduli have been obtained by several authors [8, 43–45, 51] for a *single* sinusoidally undulating membrane. Taking the membrane height profile about a flat reference plane to be $u(x) = u \sin(qx)$, $\delta\kappa^{\text{el}}$ is obtained by expanding the Poisson–Boltzmann equation about the flat reference plane, for small u and q . In refs [8, 43, 44] only the linearized Debye–Hückel regime is investigated, but refs [45, 51] considered the full non-linear Poisson–Boltzmann equation.

6.3.1. Debye–Hückel limit: strong electrolyte

Calculations have been done in the decoupled (small s) and completely coupled (large s) limits [8, 43, 44]. The results coincide with the ones done in the cylindrical geometry:

$$\begin{aligned} \delta\kappa^{\text{el}} &= \frac{3\pi}{2} \frac{\sigma^2 \lambda_{\text{D}}^3}{\varepsilon_{\text{w}}}, & \delta\kappa_{\text{G}}^{\text{el}} &= -\frac{\pi\sigma^2 \lambda_{\text{D}}^3}{\varepsilon_{\text{w}}}, & \text{decoupled,} \\ \delta\kappa^{\text{el}} &= \frac{\pi}{2} \frac{\sigma^2 \lambda_{\text{D}}^3}{\varepsilon_{\text{w}}}, & \delta\kappa_{\text{G}}^{\text{el}} &= -\frac{\pi\sigma^2 \lambda_{\text{D}}^3}{\varepsilon_{\text{w}}}, & \text{completely coupled.} \end{aligned} \tag{6.7}$$

It was shown [45], then, that eq. (6.4) also describes the general s behavior of $\delta\kappa^{\text{el}}$ for the sinusoidally undulating membrane in the long wavelength limit of $q\lambda_{\text{D}} \ll 1$.

6.3.2. Intermediate regime: weak electrolyte

The full (non-linear) Poisson–Boltzmann equation with one sinusoidally undulating membrane was considered by Fogden et al. in the decoupled limit [51]. They have shown that $\delta\kappa^{\text{el}}$ in the long wavelength limit has the same expression as the one calculated [48] in the non-linear (but decoupled) regime for the cylindrical geometry, eq. (6.6). More recently, the decoupled limit as well as the completely coupled limit have been calculated [45]. For long wavelength, $q\lambda_{\text{D}} \ll 1$, $\delta\kappa^{\text{el}}$ has the following

form:

$$\delta\kappa^{\text{el}} = \frac{\varepsilon_w T^2 \lambda_D}{2\pi e^2} \left(1 - 2(\lambda_D^{-1}b)^2 + \frac{2(\lambda_D^{-1}b)^3}{\sqrt{1 + (\lambda_D^{-1}b)^2}} \right), \quad \text{decoupled,} \quad (6.8)$$

$$\delta\kappa^{\text{el}} = \frac{\pi\sigma^2\lambda_D^3}{2\varepsilon_w} \left(\frac{2\lambda_D^{-1}b}{\lambda_D^{-1}b + \sqrt{1 + (\lambda_D^{-1}b)^2}} \right)^2, \quad \text{completely coupled.}$$

Both expressions of eq. (6.8) have the correct limits for $\lambda_D^{-1}b \gg 1$ (the Debye–Hückel region) as in eq. (6.3); and $\lambda_D^{-1}b \ll 1$ (the Intermediate region) as in eq. (6.6). The decoupled limit agrees with the one obtained in cylindrical geometry [48].

6.4. Membranes with variable surface charge density

Finally let us briefly mention the case where the surface charge density is not a constant but varies throughout the membrane. Membranes with variable surface charge density can be formed when a charged (cationic, anionic) amphiphile is mixed with a non-charged (zwitterionic) one. For example, a mixed system of phosphatidyl choline (non-charged) and phosphatidyl glycerol sodium salt (charged) [52, 53]. We discuss here electrostatic interactions only within the (simpler) linear Debye–Hückel regime.

When the charges within the membrane have a spatial distribution, two different limits can be distinguished depending on the lateral ion mobility [54]. First, for a quenched (immobile) surface charge density, $\sigma(x) = \sum \sigma_n \cos nqx$, of a membrane with one undulation mode $u(x) = u \cos qx$, the contribution to the bending modulus $\delta\kappa^{\text{el}}$ was calculated. It includes contributions from all the modes of the charge density, σ_n . For several simple $\sigma(x)$, the electrostatic interactions can be shown to rigidify the membrane since $\delta\kappa^{\text{el}} > 0$. This is a generalization of a constant surface charge distribution $\sigma(x) = \sigma_0$.

Second, for mobile charges on a flexible membrane, it has been shown [45] that the optimal surface charge density which minimizes the electrostatic free energy (in presence of an electrolyte) is identical to a membrane with an *equipotential* surface. This result assumes that the only degrees of freedoms present are the electrostatic ones. More generally, competition between electrostatic interactions and short-range inplane interactions lead to an optimal $\sigma(x)$. In this case the membrane is not anymore an equipotential surface. For asymmetric membranes, the contribution of the electrostatic interaction to the spontaneous curvature, c_0 in eq. (6.1), can be calculated. The asymmetry of the bilayer membrane can be a result of two different solvents on the two sides of the membrane, or an internal asymmetry which has to do with different structure and/or composition of the two monolayers. More details can be found in ref. [54].

Depending on the lateral diffusivity of the two components, a real membrane show a more complex and *dynamical* behavior in which the charge distribution is neither

annealed nor quenched. So the quenched and annealed charge distribution should be regarded as the two extreme limits of, respectively, very slow and very fast relaxation times within the membrane. Note that the ions in solutions are always assumed to be in thermodynamical equilibrium and will adjust their distribution according to the charge distribution on the membrane.

7. A stack of charged lamellae

Natural phospholipids or artificial surfactants dissolved in water can form lamellar phases consisting of a stack of alternating amphiphilic bilayers and water regions [50, 55, 56]. The repeated periodicity of the stack can vary from as low as a few Angstroms to as high as several thousand angstroms [49, 57, 58].

The stability of the lamellar phase with respect to other ‘disordered’ phases (e.g., spherical or cylindrical micelles, isotropic ‘sponge’ L_3 phase), or other, liquid crystalline, phases (e.g., hexagonal, cubic) depends on several system parameters: specific short range interactions, controlled by the chemistry of the amphiphiles (size and structure of the aliphatic chain), as well as on thermodynamic and electrostatic parameters (temperature, membrane surface charge, ionic strength of the aqueous solution, and relative concentrations of the various components). In some cases, the stability depends crucially on the type and amount of an added co-surfactant (usually a short chain alcohol like pentanol [57]).

These parameters change the relative importance of intra- and inter-layer interactions. For layer separation below 20 Å, Van der Waals attraction is compensated by repulsive hydration forces [11]. Hydration force plays an important role in preventing the phenomenon of *adhesion* of vesicles and membranes. These forces are reviewed elsewhere in this Handbook (Helfrich, Lipowsky, Parsegian and Rand). For large inter-membrane separations (roughly larger than a few dozens angstroms), the important interactions are attractive Van der Waals and repulsive electrostatic interactions. As was previously explained, electrostatic interactions strongly depend on the ionic strength of the solution. They can be completely screened, say for ionic strength of about 1.0 M, or only weakly screened for pure water.

7.1. Suppression of Helfrich interactions by electrostatics

Lamellar phases composed of a stack of membranes show quite universal behavior when the membrane are flexible with κ of order T . Entropically induced out-of-plane fluctuations of the stack cause an effective *long range* repulsion between adjacent membranes called the *undulation force* and have a pure entropic origin. This important idea was predicted by Helfrich in 1978 [40] and has been checked experimentally [57–59] in recent years, using high resolution X-ray scattering and dynamic light scattering. Helfrich’s prediction takes into account the loss of entropy due to the constraint that each membrane is bounded between its two adjacent neighboring membranes.

The repulsive undulation interactions between the membranes (per unit area) have the form [40]

$$f_u \simeq \frac{T^2}{\kappa} \frac{1}{d^2} \quad (7.1)$$

or equivalently the disjoining pressure $P(d) = -\partial f_u / \partial d \sim 1/d^3$, where d is the average inter-membrane separation. As is clear from eq. (7.1), the undulation interaction is dominant only when the membrane is quite flexible, $\kappa \simeq T$. In the absence of charges (for lamellar phases diluted in oil) or for a strongly screened case (strong electrolyte solution), experiments verified the functional form of the predicted $P(d)$ for a range of spacings, d [49]. In other experiments, done for strongly charged and unscreened systems (no electrolyte), the dominant repulsion comes from the electrostatic interactions between completely flat and rigid stack membranes [57].

In what follows we will consider the interplay between the electrostatics and fluctuations of a stack of membranes [60–64]. We do not include Van der Waals and hydration forces. The excess free energy (per unit area) of one lamella fluctuating about its average position $z = 0$ over a flat reference lamella is

$$f_u = f_{\text{bend}} + \Delta f_{\text{el}} \quad (7.2)$$

where f_{bend} is the inplane bending free energy, eq. (6.1), for one undulating membrane. In the limit of small fluctuations f_{bend} can be conveniently estimated as $f_{\text{bend}} \simeq \frac{1}{2} \kappa (\nabla^2 u)^2$, where $u(\vec{r})$ is the displacement field of the membrane at a point \vec{r} . The second term is the excess in electrostatic free energy due to the undulation. Within a local Deryagin-like approximation [2], Δf_{el} can be estimated by expanding the electrostatic free energy of a stack of flat membranes with separation d to second order in u ,

$$\Delta f_{\text{el}} = \frac{1}{2} \frac{\partial^2 f_{\text{el}}}{\partial d^2} u^2. \quad (7.3)$$

More formally, Δf_{el} can be expanded up to second order in u and forth order in q in the limit of large wavelengths and small amplitudes. Equation (7.3) is the zero q contribution to the u^2 term. The two other terms: $q^2 u^2$ and $q^4 u^2$ are correction to surface tension and bending modulus. Whereas the first can be dropped out for incompressible membranes, the second will be discussed later.

Substituting eq. (7.3) in (7.2) and expressing f_u as a sum over all q -modes, we obtain

$$f_u = \frac{1}{2} \kappa \sum_q u_q^2 (q^4 + \xi^{-4}) \quad (7.4)$$

where $\xi^{-4} = \kappa^{-1} \partial^2 f_{\text{el}} / \partial d^2$, or equivalently $\xi^{-4} = -\kappa^{-1} \partial P(d) / \partial d$, ξ is the in-plane electrostatic correlation length, and u_q is the q -mode of $u(x)$. This introduces a new

cutoff for the undulation modes in the small q limit [42, 60]. For strong electrostatic interactions this new cutoff can dominate over the cutoff introduced by Helfrich for the uncharged case (the inter-membrane distance d) in order to preserve the lamellar order of the stack. We will estimate ξ by looking at the various limits for f_{el} for two flat and charged membranes (see section 4 and fig. 5).

Assuming that we are in the small fluctuation limit, the root-mean-square fluctuation $\sqrt{\langle u^2 \rangle}$ is much smaller than d . We later will check which of the electrostatic limits satisfies this condition: $\langle u^2 \rangle \ll d^2$. Using the equipartition theorem for the energy modes we get

$$\langle u^2 \rangle = \frac{T}{\kappa} \sum_q \frac{1}{q^4 + \xi^{-4}} = \frac{T}{8\kappa} \xi^2. \quad (7.5)$$

In the Gouy–Chapman region, the electrostatic interactions are almost unscreened since $d/\lambda_D \ll 1$. Using eq. (4.17) for the free energy of the two flat membranes, ξ is calculated to be [60, 61],

$$\xi = d \left(\frac{\kappa l}{\pi T d} \right)^{1/4} \sim d^{3/4} \quad (7.6)$$

leading to an estimate for $\langle u^2 \rangle$:

$$\langle u^2 \rangle = \left(\frac{T}{\kappa} \frac{l}{\pi d} \right)^{1/2} \frac{d^2}{8}. \quad (7.7)$$

We see from the above equation that for flexible membranes in a dilute lamellar phase $\kappa \simeq T$ and $d \gg l \simeq 7 \text{ \AA}$, indeed $\langle u^2 \rangle \ll d^2$, as is expected in the strong electrostatic regime since electrostatic interactions suppress the small q fluctuations. In addition, we can estimate the ratio f_u/f_{el} of the electrostatic and undulatory parts of the free energy: $f_{\text{el}} = \pi T/2ld$ and $f_u = T/8\xi^2$

$$f_u/f_{\text{el}} = \frac{1}{4\pi} \frac{ld}{\xi^2} \simeq \left(\frac{Tl}{\kappa d} \right)^{1/2} \ll 1. \quad (7.8)$$

Therefore, in the Gouy–Chapman regime because of strong and unscreened electrostatic interactions, the steric repulsion between neighboring membranes is small compared with the electrostatic contribution which suppresses the spectrum of out-of-plane fluctuations to values below the inter-membrane separation d [60, 61]. This is in agreement with the experimental findings which found that in the strong electrostatic regime, the data did not show any influence of the Helfrich steric interactions. Electrostatic interactions by themselves gave the best fit [57]. Note that in eqs (7.6)–(7.8) above we did not insert explicitly the electrostatic contribution to the bending modulus, $\delta\kappa^{\text{el}}$. This contribution in lamellar phases will be discussed in the next section.

In the other (weaker) electrostatic regimes, fig. 5, the suppression of the fluctuations is less drastic and in some cases, the screened electrostatic interactions can be completely neglected. Using eqs (4.24), (4.21) and (4.15) for the Debye–Hückel, Intermediate and ideal-gas regions, respectively, we obtain [60]:

$$\begin{aligned}\xi &= \left(\frac{\pi l \kappa \lambda_D^3}{8T} \right)^{1/4} e^{d/4\lambda_D} \quad \text{Debye–Hückel,} \\ \xi &= \left(\frac{\pi l b^2 \kappa \lambda_D}{2T} \right)^{1/4} e^{d/4\lambda_D} \quad \text{Intermediate,} \\ \xi &= \left(\frac{\pi \kappa b l}{T} \right)^{1/4} d^{1/2} \quad \text{ideal-gas.}\end{aligned}\tag{7.9}$$

Clearly for $d/\lambda_D \gg 1$, the Debye–Hückel and Intermediate results for ξ depend exponentially on d/λ_D leading to $\xi \gg d$. Hence, for these weak electrostatic cases, the new electrostatic cutoff will not suppress substantially the out-of-plane fluctuations. It does play only a minor role in reducing the Helfrich steric repulsion between adjacent membranes as compared with the uncharged case. Imposing the constraint $\langle u^2 \rangle \simeq d^2$ we get the following expression for f_u :

$$f_u \simeq \frac{T^2}{\kappa(d - 2\lambda_D)^2} \left[1 - \text{const} \left(\frac{\kappa}{T} \right)^2 \left(\frac{d}{\xi} \right)^4 \right]\tag{7.10}$$

where the prefactor of the second term is a constant depending on the details of the approximation employed. Thus, as long as $d/\lambda_D \gg 1$, the electrostatic interactions only slightly modify the Helfrich steric interactions. The main correction is that the effective distance between adjacent membranes is reduced to $d - 2\lambda_D$ instead of d . This is the conclusion for both the Debye–Hückel and Intermediate regimes. The ideal-gas regime is somewhat more delicate. As long as $bl < d^2$ but $b > d$, ξ is smaller than d and fluctuations are suppressed.

7.2. Rigidity of charged lamellae

Another important issue to consider for a stack of charged lamellae is how much electrostatic interactions affect the bending rigidity. In the previous section we reviewed the effect of electrostatic interactions on the spectrum of out-of-plane fluctuations of the membrane and its relation to the Helfrich interactions. An electrostatic contribution to the bending modulus κ will also have an effect on the spectrum of fluctuations and on structural properties. This contribution can, in principle, be measured experimentally [49, 59].

We recall that the electrostatic contribution to the bending modulus, $\delta\kappa^{\text{el}}$, has been presented in section 6 for a single lamella (one membrane). For a stack of membranes this applies in the limit where the inter-lamella spacing d is very large compared with the other electrostatic lengths: b and λ_D . When d is not that large,

the electrostatic contribution to the bending modulus, $\delta\kappa^{\text{el}}$, depends also on d . We will present calculations of $\delta\kappa^{\text{el}}$ in the different electrostatic limits corresponding to the regions of fig. 5, since the full calculation of $\delta\kappa^{\text{el}}$ is extremely complex and not available at present.

Most of the calculations for $\delta\kappa^{\text{el}}$ have been done in the decoupled electrostatic limit (see section 6 for more details). Three types of geometries have been considered:

- (i) Two concentric cylinders (or spheres) in the limit of large radii of curvature, R_1 and R_2 , and small separation, $d/R_1 \ll 1$, and $d/R_2 \ll 1$ where $d = R_2 - R_1$ as in fig. 7.
- (ii) Two undulating membranes with an average separation d and a relative phase shift θ , each undulating with an amplitude u and a wavenumber q :

$$u_1 = \frac{d}{2} + u \cos qx \quad \text{and} \quad u_2 = -\frac{d}{2} + \cos(qx + \theta). \quad (7.11)$$

The two extreme phase shifts between the two membranes are either an in-phase ‘capillary mode’ with $\theta = 0$, or an out-of-phase ‘breathing mode’ with $\theta = \pi$ as in fig. 8.

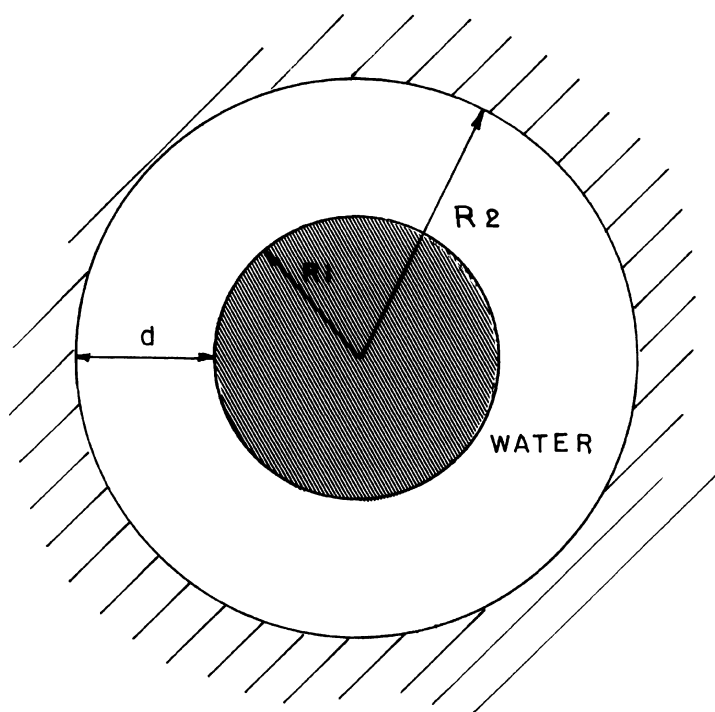


Fig. 7. Schematic drawing of a cross-section through two concentric cylindrical membranes of radii R_1 and R_2 . The aqueous solution fills the spacing of thickness $d = R_2 - R_1$ between the two membrane. This geometry is used to calculate $\delta\kappa^{\text{el}}$ in the limit of $R_1/d \gg 1$ and $R_2/d \gg 1$. Notice that an added complication as compared with two flat surfaces (fig. 4) is that the electric field is not zero at the midplane $(R_1 + R_2)/2$, due to the overall curvature of the cylinders.

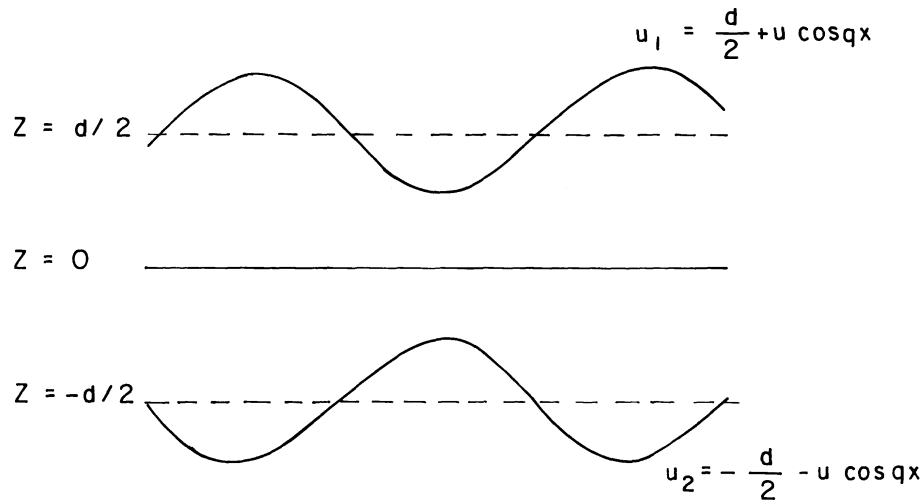


Fig. 8. Schematic drawing of two membranes u_1 and $u_2 = -u_1$, undulating out-of-phase about $z = d/2$ and $z = -d/2$, respectively. The wavenumber and amplitude of the undulations are q and u , respectively.

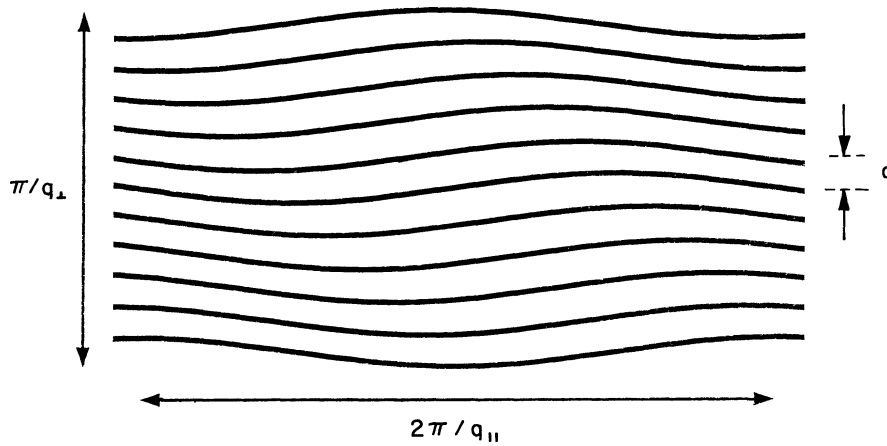


Fig. 9. Sketch of a stack of undulating charged membranes. Membranes are assumed to have average inter-membrane separation d , and undulations of wavelength $2\pi/q_{||}$ and relative phase dq_{\perp} . Undulation amplitudes are shown exaggerated for effect; actual membranes are assumed to have low amplitude ($u \ll d$), long wavelength fluctuations ($q_{||}d \ll 1$) with small inter-membrane phase angle ($q_{\perp}d \ll 1$).

- (iii) In analogy to smectic liquid crystals, a continuum approximation for the layered lamellar phase where the density of the lamellae is assumed to be a slowly varying and periodic function both in the x direction (parallel to the lamellae), and in the z direction (perpendicular to the lamellae) as is seen in fig. 9.

7.2.1. Membrane rigidity in the Gouy–Chapman region

In terms of the regions of fig. 5, the single membrane calculations of section 6 gave us the contribution $\delta\kappa^{\text{el}}$ for the large-spacing Debye–Hückel regime (region I), eq. (6.4), and in the non-linear Intermediate regime, eq. (6.8). In the Gouy–Chapman regime of strong surface charge, large-spacing and no screening: $bd \ll 1$, and $d/\lambda_D \ll 1$, the effect of electrostatics is expected to be the largest. The scaling form for $\delta\kappa^{\text{el}}$ was conjectured by Pincus et al. [60] and later calculated by Higgs and Joanny [65]. The scaling form can be easily obtained by requiring a smooth crossover between the Intermediate and Gouy–Chapman regions on the crossover line $\lambda_D = d$. Since $\delta\kappa^{\text{el}} \sim \lambda_D$ in the Intermediate region, eq. (6.8), this implies $\delta\kappa^{\text{el}} \simeq Td/l$. Note that the expression for the pressure $P(d)$ also crosses over smoothly from the intermediate region, eq. (4.21), to the Gouy–Chapman one, eq. (4.17) on the same line, $d/\lambda_D \simeq 1$.

Higgs and Joanny [65] calculated $\delta\kappa^{\text{el}}$ using two different systems. In the first, two weakly undulating membranes with an out-of-phase phase shift of $\theta = \pi$ are considered (fig. 8). The non-linear Poisson–Boltzmann equation (2.4) in the limit of no-added electrolyte is solved with two undulating boundaries: $u_1 = d/2 + u \cos qx$ and $u_2 = -d/2 - u \cos qx$ while requiring $u \ll d$. Because of the symmetry about the midplane, $z = 0$, for the out-of-plane mode, it is enough to solve the Poisson–Boltzmann equation in the interval $[0, d/2]$ with a constant surface charge density σ at $z = d/2$ and a vanishing electric field at $z = 0$. The pressure $P(d)$ is calculated by taking the variation of the free energy f_{el} with respect to d , eq. (2.8), in the limit of no-added electrolyte

$$P(d) = \int \left(Tn(0) + \frac{\varepsilon_w}{4\pi} \psi(0, x) \frac{\partial E_x(0, x)}{\partial d} \right) dx \quad (7.12)$$

where the integral is performed along the midplane $z = 0$, and E_x is the x component of the electric field. Expanding the potential ψ and the pressure $P(d)$ up to order $u^2 q^4$ for the Gouy–Chapman region ($b \ll d$), the contribution to the bending modulus has been shown to scale as

$$\delta\kappa^{\text{el}} \simeq \text{const } T \frac{d}{l} \quad \text{for } b \ll d \ll \lambda_D. \quad (7.13)$$

The prefactor in (7.13) was not calculated for two undulating membranes due to mathematical complexity. However, this prefactor was calculated by the same authors [65] in a different geometry of two concentric cylindrical membranes of radii R_1 and R_2 , respectively (fig. 7). Note that here the midplane of an average radius $R = (R_1 + R_2)/2$ is not a plane of vanishing electric field due to the overall curvature. The electric potential of the double layer problem between two concentric cylinders was calculated some time ago in a seminal paper by Fuoss et al. [66] in relation to their model of polyelectrolytes. This expression for ψ was used in ref. [65] to calculate the pressure $P(d)$, eq. (7.12), as an expansion to second order in $1/R$. In the limit of $d/R \ll 1$, the bending constant can be deduced from this expansion

$$\delta\kappa^{\text{el}} = T \left(\frac{1}{\pi} - \frac{\pi}{12} \right) \frac{d}{l} \simeq 0.06 T \frac{d}{l}. \quad (7.14)$$

Again, eq. (7.14) is valid only in the limit of no-added electrolyte, $d/\lambda_D \ll 1$, and strong surface charge, $b \ll d$, which exists as a limit of the Gouy–Chapman region, fig. 5.

7.2.2. Membrane rigidity in the ideal-gas region

We turn now to ideal-gas region which is a region of weakly charged membranes but also with weak electrolytes. Harden et al. [67] calculated $\delta\kappa^{\text{el}}$ in this case for two concentric cylinders very much along the lines described in the previous section for the Gouy–Chapman region. The difference is that for the ideal-gas case $b/d \gg 1$, although the same limit of no-added electrolyte is taken (very large λ_D). The result in the ideal-gas regime is:

$$\delta\kappa^{\text{el}} = \frac{1}{30\pi} \frac{T}{b^2 l} d^3. \quad (7.15)$$

Note that the scaling behavior of $\delta\kappa^{\text{el}} \sim d^3/b^2$ in the ideal-gas region crosses over smoothly to the result for the Gouy–Chapman region, $\delta\kappa^{\text{el}} \sim d$ from eq. (7.14), on the boundary line $b = d$.

7.2.3. Membrane rigidity in the small-spacing Debye–Hückel region

Since the Debye–Hückel limit is the linear limit of the Poisson–Boltzmann equation, the free energy can be handled easier in a variety of boundary conditions. The contribution to $\delta\kappa^{\text{el}}$ in this Debye–Hückel limit for *one* single membrane have been described in section 6 with the result: $\delta\kappa^{\text{el}} = 3T\lambda_D^3/(4\pi lb^2)$ (taking into account the *two* sides of the membrane). This scaling corresponds to the large-spacing Debye–Hückel region (marked as region I in fig. 5) where $\lambda_D/d \ll 1$ and $b/\lambda_D \gg 1$.

The small-spacing Debye–Hückel regime is defined in the wedge $\lambda_D/d \gg 1$ but $b/d \gg (\lambda_D/d)^2$ (marked as region II in fig. 5). The first inequality is the condition on the short distance region, whereas the second is the condition on the linearity of the Poisson–Boltzmann equation. Pincus et al. [60] have studied the general Debye–Hückel case for two membranes, $u_1 = d/2 + u \cos qx$ and $u_2 = -d/2 - u \cos qx$ which fluctuate out-of-phase one with respect to the other in a breathing mode (so-called *peristaltic mode*) as shown on fig. 8). It is important to note that the membranes are taken to have a frozen spatial configuration; namely, q and u are both fixed. In the limit of small-spacing Debye–Hückel, [$\lambda_D/d \gg 1$; $b/d \gg (\lambda_D/d)^2$], $\delta\kappa^{\text{el}}$ is found to be

$$\delta\kappa^{\text{el}} \simeq \frac{T\lambda_D^3}{lb^2} \left(\frac{\lambda_D}{d} \right)^3 \quad (7.16)$$

which scales with an extra factor of $(\lambda_D/d)^3$ than the result for the large-spacing Debye–Hückel, eq. (6.3). We discuss below the limitations of this approach [67] when applied to a stack of undulating lamellae.

The bending constant was also calculated for a different electrostatic boundary condition of *constant surface potential* [8]. The free energy is calculated for two

equipotential surfaces (membranes with a constant surface potential ψ_s) undulating with a fixed q -mode and with a general phase shift θ between them. The calculations are restricted to the linear Debye–Hückel regime. In the small-spacing Debye–Hückel limit, $\delta\kappa^{\text{el}}$ can be evaluated from their result to be

$$\delta\kappa^{\text{el}} = \frac{\varepsilon_w \psi_s^2 \lambda_D}{90} \left(\frac{d}{2\lambda_D} \right)^5 (16 - 7 \cos \theta) \quad (7.17)$$

where ψ_s is the fixed surface potential.

Although the above results, eqs (7.16) and (7.17) are valid for two membranes of a fixed spatial undulation, it was pointed out [67] that the connection to a stack of lamellae – as is measured in experiments – *is not precise especially in the small-spacing limit*. The reason is that taking a configuration of charged membranes undulating out-of-phase contributes to the bulk modulus in addition to the bending terms.

The way $\delta\kappa^{\text{el}}$ was calculated for a stack of membranes (lamellar phase) [67] was to consider the stack in the long wavelength and small amplitude limit. The spatial undulation field is written as $u(x, z) = u \cos(q_{\parallel}x + q_{\perp}z)$, where both $q_{\parallel}d \ll 1$ and $q_{\perp}d \ll 1$ as can be seen in fig. 9. Calculating the electrostatic free energy and expanding it to second order in the mode amplitude u , we can identify $\delta\kappa^{\text{el}}$ as the coefficient of the $q_{\perp}^4 u^2$ term

$$\delta\kappa^{\text{el}} = \frac{1}{30\pi} \frac{T}{b^2 l} d^3. \quad (7.18)$$

Note that this result in the small-spacing Debye–Hückel for a undulating stack agrees *exactly* with the result for $\delta\kappa^{\text{el}}$ in the ideal-gas regime. Moreover, it also agrees with a calculation of $\delta\kappa^{\text{el}}$ using two concentric charged cylinders configuration.

This ends the presentation of the electrostatic contribution to the bending rigidity in the various electrostatic regimes. In fig. 10 (a) and (b), we plotted the expected scaling of $\delta\kappa^{\text{el}}$ of a stack of membranes in a lamellar phase as function of the Debye–Hückel screening length λ_D in the limit of weakly and strongly charged membranes, respectively. The figure shows a crossover in the scaling of $\delta\kappa^{\text{el}}$ depending on the various electrostatic regimes. The contribution to κ is the strongest for the least screened interactions when λ_D becomes large. Such scans can be verified experimentally by changing the strength of the electrolyte. Other possible scans will be changing the membrane spacing d or the strength of the surface charge $\sigma \sim 1/b$ by mixing together charged and non-charged (zwitterionic) amphiphiles.

8. Conclusions and future prospects

Research on the electric double layer problem started at the beginning of the century with the pioneering works of Gouy, Chapman, Debye and Hückel. Within a continuum approach (Poisson–Boltzmann theory), the electrostatics of *rigid* bodies

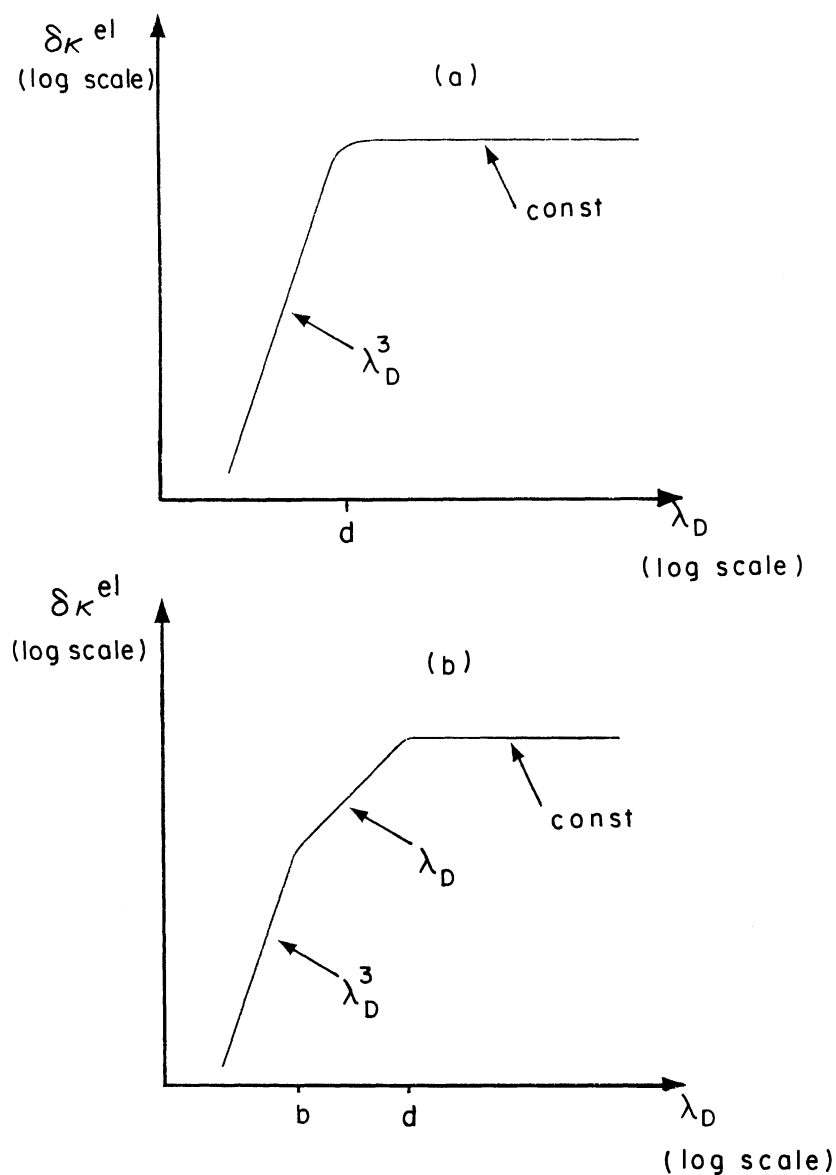


Fig. 10. Sketch of electrostatic contribution to the membrane bending modulus $\delta\kappa^{el}$ as a function of the Debye-Hückel screening length λ_D at fixed d and b . In (a), we show the case of weakly charged membranes, $b < d$. With increasing λ_D , $\delta\kappa^{el}$ first scales as λ_D^3 and then crosses over to a constant value for $\lambda_D > d$. In (b) we show the analogous plot for strongly charged membranes. In this case after an initial regime of $\delta\kappa^{el} \sim \lambda_D^3$, $\delta\kappa^{el}$ first crosses over to a linear regime, $\delta\kappa^{el} \sim \lambda_D$ at $\lambda_D > b$ followed by a second crossover to a constant value for $\lambda_D > d$. Adapted from ref. [67].

immersed in ionic solutions is well understood. This approach was used quite successfully to investigate stability of colloidal dispersion, charged micelles and model membranes, and even polyelectrolytes. In recent years, other theories taking into account the discreteness of the charges and correlations have been developed but mainly in the simpler planar geometry. Some of the findings that cannot be explained within the Poisson–Boltzmann theory are the behavior of divalent ions like Ca^{++} which in some cases can induce an attractive interaction between membranes, and to non-monotonous profiles of the counterions in the proximity of the charge surfaces (up to a few angstroms away). Beside these points, it has been shown in numerous studies that the Poisson–Boltzmann theory is actually quite reliable.

For flexible and *heterogeneous* structures like membranes, the interplay between electrostatics and structure is far less understood because of the complexity of the problem involved. The electrostatics degrees of freedom are coupled to the membrane shape. Hence, one has to solve the electrostatic problem with variable boundary conditions in a self-consistent way. This is a tremendous task and only first attempts in this direction have been undertaken.

By considering the membrane as a flexible (and *homogeneous*) interface, the contribution of the charges to the bending moduli has been found in various electrostatic regimes (screened, unscreened, etc.). Electrostatics tends to rigidify the membranes and also suppresses the out-of-plane fluctuations of a lamellar phase composed of a stack of membranes. However, when the membrane is heterogeneous (e.g., composed of two components), electrostatics can induce shape instabilities in relation to a lateral segregation of the two components.

In the future more complex models will, hopefully, be studied in order to make closer contact with biological membranes. Mixtures of charged and zwitterionic phospholipids, interactions between charged lipids and membrane proteins, biopolymers or other short-chain impurities are all of great importance in biological systems. When considering membranes as multi-component systems, it will be necessary to include other interactions as Van der Waals and hydration and to understand the interplay between those interactions and the electrostatic ones. Finally, even when the membrane is not charged it is composed of phospholipids which have a polar head. Dipole-dipole interactions are also of importance as they can lead to formation of dipolar domains and influence many of the membrane properties.

All of the above represent very challenging problems for future investigations. From the fundamental point of view, they relate to the physics of charged, flexible and heterogeneous structures. In addition, they can provide a better understanding of complex biological systems.

Acknowledgments

I would like to thank I. Borukhov, H. Diamant, G. Guttman, J.F. Joanny, S. Marcelja and A. Parsegian for comments and critical reading of this chapter. A part of the theoretical results presented here have been obtained in collaboration with G. Guttman, J. Harden, J.F. Joanny, C. Marques and P. Pincus. Partial support from the Israel Academy of Sciences and Humanities and the German-Israel Binational Foundation (GIF) under grant No. I-0197 is gratefully acknowledged.

References

1. Verwey, E.J.W. and J.Th.G. Overbeek, 1948, *Theory of the Stability of Lyophobic Colloids* (Elsevier, New York).
2. Israelachvili, J.N., 1990, *Intermolecular and Surface Forces* (Academic Press, London).
3. Gouy, G., 1910, *J. Phys. (France)* **9**, 457.
Gouy, G., 1917, *Ann. Phys. (Leipzig)* **7**, 129.
4. Chapman, D. L., 1913, *Philos. Mag.* **25**, 475.
5. Debye, P. and E. Hückel, 1923, *Physik Z.* **24**, 185.
Debye, P. and E. Hückel, 1923, *Physik Z.* **25**, 97.
6. Ninham, B.W. and V.A. Parsegian, 1971, *J. Theoret. Biol.* **31**, 405.
7. Kékicheff, P., S. Marcelja, T.J. Senden and V.E. Shubin, 1993, *J. Chem. Phys.* **99**, 6098.
8. Goldstein, R.E., A.I. Pesci and V. Romero-Rochin, 1990, *Phys. Rev. A* **41**, 5504.
9. Mahatny, J. and B.W. Ninham, 1976, *Dispersion Forces* (Academic, New York).
10. Tanford, C., 1980, *The Hydrophobic Effect* (Wiley, New York).
11. Parsegian, V.A., N. Fuller and R.P. Rand, 1979, *Proc. Nat. Acad. Sci. USA* **76**, 2750.
Rand, R.P., 1981, *Annu. Rev. Biophys. Bioeng.* **10**, 277.
12. Attard, P., D.J. Mitchell and B.W. Ninham, 1988, *J. Chem. Phys.* **88**, 4987.
13. Attard, P., D.J. Mitchell and B.W. Ninham, 1988, *J. Chem. Phys.* **89**, 4358.
14. For a review see: Marcelja, S., 1990, in: *Liquids at Interfaces*, eds J. Charvolin, J.F. Joanny and J. Zinn-Justin (North-Holland, Amsterdam).
15. Kjellander, R. and S. Marcelja, 1985, *J. Chem. Phys.* **82**, 2122.
16. Kjellander, R., T. Akersson, B. Jönsson and S. Marcelja, 1992, *J. Chem. Phys.* **97**, 1424.
17. Marcelja, S., 1992, *Biophys. J.* **61**, 1117.
18. Shubin, V.E. and P. Kékicheff, 1993, *J. Colloid Interface Sci.* **155**, 108.
19. McLaughlin, S.G.L., 1989, *Ann. Rev. Biophys. Biophys. Chem.* **18**, 113.
20. Hiemenz, P.C., 1977, *Principles of Colloid and Surface Chemistry* (Dekker, New York).
21. Stern, O., 1924, *Z. Elektrochem.* **30**, 508.
22. Kiometzis, M. and H. Kleinert, 1989, *Phys. Lett. A* **140**, 520.
23. Winterhalter, M. and W. Helfrich, 1992, *J. Phys. Chem.* **96**, 327.
24. For membranes with non-equal charges, see, e.g., Parsegian, V.A. and D. Gingell, 1972, *Biophys. J.* **12**, 1192.
25. Parsegian, V.A., 1966, *J. Chem. Soc. Faraday Trans.* **62**, 848.
26. Cowley, A.C., N.L. Fuller, R.P. Rand and V.A. Parsegian, 1978, *Biochemistry* **17**, 3163.
27. Langmuir, I., 1938, *J. Chem. Phys.* **6**, 873.
28. Guttman, G., 1992, M. Sci. Thesis, Tel Aviv University (unpublished).
29. Helfrich, W., 1973, *Z. Naturforsch.* **28c**, 693.
30. David, F., 1989, in: *Statistical Mechanics of Membranes and Surfaces*, Vol. 5, eds D. Nelson, T. Piran, S. Weinberg (World Scientific, Singapore).
31. Goldstein, R.E. and S. Leibler, 1989, *Phys. Rev. A* **40**, 1025.
32. Leibler, S. and D. Andelman, 1987, *J. Phys. (Paris)* **48**, 2013.
33. Janiak, M.J., D.M. Small and G.G. Shipley, 1979, *J. Biol. Chem.* **254**, 6068.
34. Findlay, E.J. and P.G. Barton, 1978, *Biochemistry* **17**, 2400.
35. Gebhardt, C., H. Gruler and E. Sackmann, 1977, *Z. Naturforsch.* **32c**, 581.
36. Wack, D.C. and W.W. Webb, 1988, *Phys. Rev. Lett.* **61**, 1210.
37. De Gennes, P.G., 1979, *Scaling Concepts in Polymer Physics* (Cornell University, Ithaca).
38. Odijk, T., 1977, *J. Polym. Sci. Phys. Ed.* **15**, 477.
39. Hofmann, S., A. Rauscher and H. Hoffmann, 1991, *Ber. Bunsenges. Phys. Chem.* **95**, 153.
40. Helfrich, W. and R.M. Servuss, 1984, *Il Nuovo Cimento* **3D**, 137. See also W. Helfrich, 1978, *Z. Naturforsch.* **33a**, 305.
41. Schulman, J.H. and J.B. Montagne, 1961, *Ann. NY Acad. Sci.* **92**, 366.
42. de Gennes, P.G. and C. Taupin, 1982, *J. Phys. Chem.* **86**, 2294.
43. Duplantier, B., R.E. Goldstein, A.I. Pesci and V. Romero-Rochin, 1990, *Phys. Rev. Lett.* **65**, 508.
Duplantier B., 1990, *Physica A* **168**, 179.
44. Bensimon, D., F. David, S. Leibler and A. Pumir, 1990, *J. Phys. (France)* **51**, 689.

45. Fogden, A. and B.W. Ninham, 1991, *Langmuir* **7**, 590.
46. Winterhalter, M. and W. Helfrich, 1988, *J. Phys. Chem.* **92**, 6865.
47. Lekkerkerker, H.N.W., 1989, *Physica A* **159**, 319.
48. Mitchell, D.J. and B.W. Ninham, 1989, *Langmuir* **5**, 1121.
49. Roux, D. and C.R. Safinya, 1988, *J. Phys. (France)* **49**, 307.
50. Meunier, J., D. Langevin and N. Boccarra (eds), 1987, *Physics of Amphiphilic Layers* (Springer-Verlag, Berlin).
51. Fogden, A., D.J. Mitchell and B.W. Ninham, 1990, *Langmuir* **6**, 159.
52. Swanson, J.E. and G.W. Feigenson, 1990, *Biochemistry* **29**, 82.
53. Feigenson, G.W., 1989, *Biochemistry* **28**, 1270.
54. Guttman, G. and D. Andelman, 1993, *J. Phys. II (France)* **3**, 1411.
55. Safinya, C.R., S.A. Safran and P.A. Pincus (eds), 1990, *Macromolecular Liquids*, *Mat. Res. Soc. Pub.* **177**.
56. Sirota, E.B., D. Weitz, T. Witten and J.N. Israelachvili (eds), 1992, *Complex Fluids*, *Mat. Res. Soc. Pub.* **248**.
57. Safinya, C.R., 1990, in: *Phase Transitions in Soft Condensed Matter*, eds T. Riste and D. Sherrington (Plenum, New York).
58. Larché, F., J. Appell, G. Porte, P. Bassereau and J. Marignan, 1986, *Phys. Rev. Lett.* **56**, 1700.
59. Nallet, F., D. Roux and J. Prost, 1989, *Phys. Rev. Lett.* **62**, 276.
Nallet F., D. Roux and J. Prost, 1989, *J. Phys. (France)* **50**, 3147.
60. Pincus, P., J.-F. Joanny and D. Andelman, 1990, *Europhys. Lett.* **11**, 763.
61. Leibler, S. and R. Lipowsky, 1987, *Phys. Rev. B* **35**, 7004. See also Lipowsky, R. and S. Leibler, 1987, in: *Physics of Amphiphilic Layers*, eds J. Meunier, D. Langevin and N. Bocarra (Springer, Berlin).
62. Evans, E.A. and V.A. Parsegian, 1986, *Proc. Nat. Acad. Sci. (USA)* **83**, 7132.
63. Podgornik, R. and V.A. Parsegian, 1992, *Langmuir* **8**, 557.
64. Evans, E.A. and I. Ipsen, 1991, *Electrochim. Acta* **36**, 1735.
65. Higgs, P.G. and J.-F. Joanny, 1990, *J. Phys. (France)* **51**, 2307.
66. Fuoss, R.M., A. Katchalsky and S. Lifson, 1951, *Proc. Nat. Acad. Sci. USA* **37**, 579.
67. Harden, J.L., C. Marques, J.-F. Joanny and D. Andelman, 1992, *Langmuir* **8**, 1170.